CHAPTER

5

THE DRAINAGE BASIN—DEVELOPMENT, MORPHOMETRY, AND HYDROLOGY

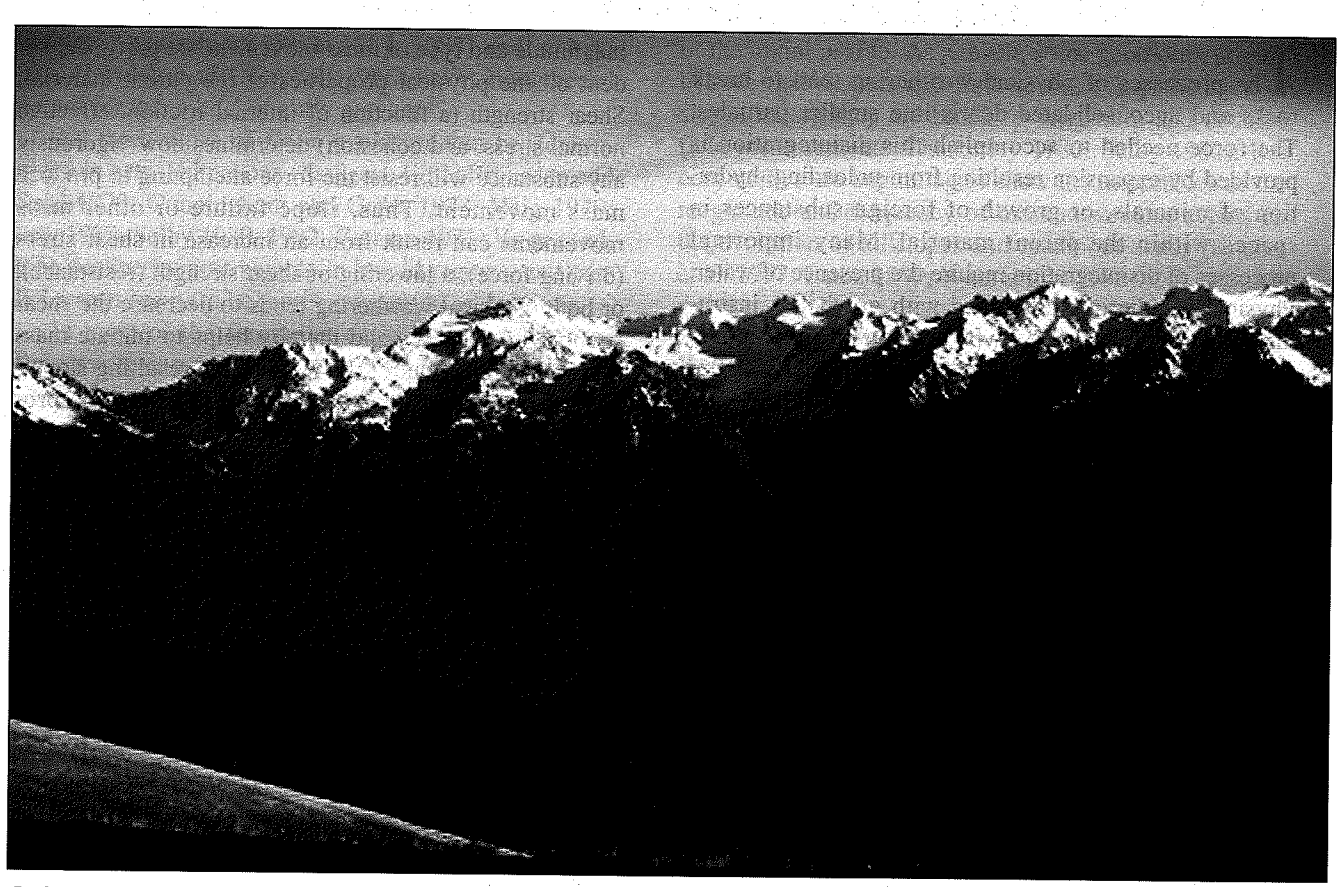

R. Craig Kochel

Figure 5.1A
An oblique aerial photo of drainage basins formed in volcanic rocks of the Oregon Cascade Range.
(Photo by R. C. Kochel)

INTRODUCTION

Two basic generalizations about rivers were realized long before geomorphology emerged as an organized science: (1) streams form the valleys in which they flow, and (2) every river consists of a major trunk segment fed by a number of mutually adjusted branches that diminish in size away from the main stem. The many tributaries define a network of channels that drain water from a discernible, finite area which is the **drainage basin,** or **watershed,** of the trunk river.

The drainage basin is the fundamental landscape unit concerned with the collection and distribution of water and sediment. Each basin is separated from its neighbor by a **divide,** or **interfluve.** (fig. 5.1A). Thus, the basin can be viewed as a geomorphic system or unit. As we will soon see, the basin is inexorably linked with hillslope processes that contribute water and sediment to the channel network in accord with the regional climate, underlying bedrock and tectonic regime, and land use by humans (fig. 5.1B). Any feature or portion of the basin can be considered a subsystem having its own unique set of processes, geology, and energy gains and losses. Furthermore, because it is possible to measure the amount of water entering the basin as precipitation and the volume leaving the basin as stream discharge, hydrologic events can be readily analyzed on a basinal scale. Likewise, much of the sediment produced within the basin is ultimately exported from the basin through the trunk river. Thus, considered on a long temporal scale, the rate of lowering of the basin surface can be estimated.

The output from a given basin compartment serves as input to the master channel and influences downstream channel characteristics and hydrologic processes in rivers. The mechanics of fluvial processes usually reflect some balance between the amount of sediment supplied for transport and the water available to accomplish this task. Throughout the discussion of drainage basins and fluvial systems, we will frequently refer to the concepts illustrated in figure 5.1B as we describe the interrelationships between various components of the fluvial system and the regulatory influence of the external variables of water and sediment in the adjustment and evolution of basins and channels.

Most Earth scientists are introduced to watersheds when they learn that drainage patterns or individual stream patterns commonly mirror certain traits of the

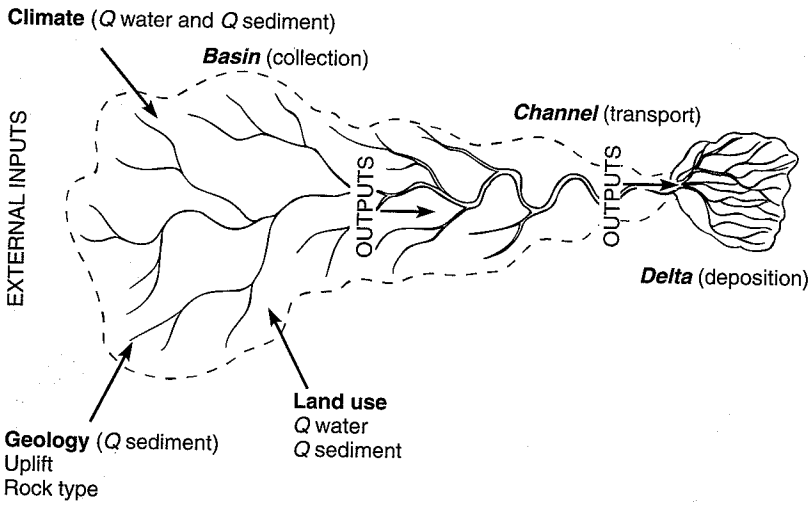

Figure 5.1B
Schematic surface components of the fluvial system. The tributaries provide links between lithology and climate and are adjusted to both. Channel characteristics vary in response to the external variables of sediment and water discharge (Q), which are influenced naturally from climate, tectonic, and lithologic factors. Human influence also modifies these variables through land use alterations.

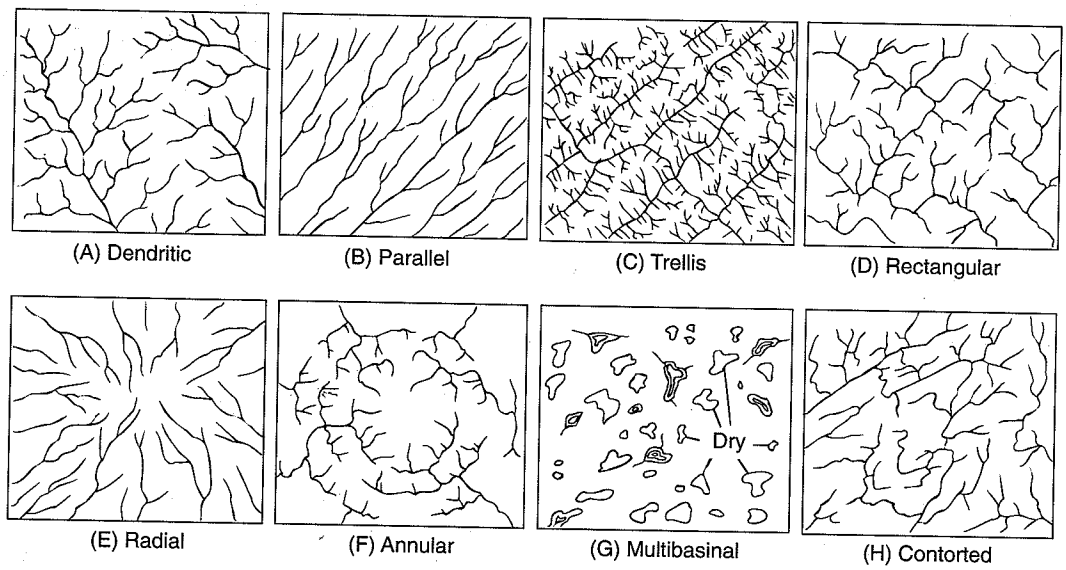

Figure 5.2A
Basic drainage patterns. Descriptions are given in table 5.1.
(Howard 1967, reprinted by permission)

underlying geology, described in figure 5.2A and table 5.1. Because the gross character of these patterns is evident on topographic maps and aerial photos, the patterns are useful for structural interpretation (fig. 5.2B) (Howard 1967) and for approximating lithology in a study of regional geology.

In a hydrologic sense, however, prior to World War II most basins were described in qualitative terms such as well-drained or poorly drained, or they were connoted descriptively in the Davisian scheme as youthful, mature, or old. The mechanics of how river channels or networks actually form and how water gets into a channel was poorly understood by geologists and hydrologists alike. This early twentieth-century view of streams and drainages contrasts markedly with the avant-garde approach presented by R. E. Horton during the latter part of this period (Horton 1933, 1945). His attempt to explain stream origins in mathematical terms and to describe basin hydrology as a function of statistical laws marked the birth of quantitative geomorphology. We now know that many of Horton's original ideas are only partially correct. Still, modern geomorphic analysis of drainage basins has its roots in Horton's original work, and his thinking has been instrumental in the development of modern geomorphology.

TABLE 5.1 Descriptions and Characteristics of Basic Drainage Patterns Illustrated in Figure 5.2A.

Pattern	Geological Significance
Dendritic	Horizontal sediments or beveled, uniformly resistant, crystalline rocks. Gentle regional slope at present or at time of drainage inception. Type pattern resembles spreading oak or chestnut tree.
Parallel	Generally indicates moderate to steep slopes but also found in areas of parallel, elongate landforms. All transitions possible between this pattern and dendritic and trellis patterns.
Trellis	Dipping or folded sedimentary, volcanic, or low-grade metasedimentary rocks; areas of parallel fractures; exposed lake or seafloors ribbed by beach ridges. All transitions to parallel pattern. Pattern is regarded here as one in which small tributaries are essentially same size on opposite sides of long parallel subsequent streams.
Rectangular	Joints and/or faults at right angles. Lacks orderly repetitive quality of trellis pattern; streams and divides lack regional continuity.
Radial	Volcanoes, domes, and erosion residuals. A complex of radial patterns in a volcanic field might be called multiradial.
Annular	Structural domes and basins, diatremes, and possibly stocks.
Multibasinal	Hummocky surficial deposits; differentially scoured or deflated bedrock; areas of recent volcanism, limestone solution, and permafrost. This descriptive term is suggested for all multiple-depression patterns whose exact origins are unknown.
Contorted	Contorted, coarsely layered metamorphic rocks. Dikes, veins, and migmatized bands provide the resistant layers in some areas. Pattern differs from recurved trellis in lack of regional orderliness, discontinuity of ridges and valleys, and generally smaller scale.

From Howard 1967, reprinted by permission.

Figure 5.2B
Trellis drainage formed as a result of the alternation of resistant rocks in the central Pennsylvania Valley and Ridge province. View is along the Susquehanna River north of Harrisburg, PA and shows sandstone ridges (resistant) and intervening valleys underlain by shale and limestone (less resistant) in this plunging syncline.
(Photo by R. Craig Kochel)

SLOPE HYDROLOGY AND RUNOFF GENERATION

The ultimate source of river flow is, of course, precipitation, which represents the major influx of water to any drainage basin. Precisely how much of that precipitation actually becomes part of the streamflow and what route a particular drop of water follows to reach a channel are topics of great concern to hydrologists. The components of the slope hydrological cycle (fig. 5.3) are the pathways of water to the streams.

Rainfall seldom makes direct contact with the bedrock or soil surface except in arid regions characterized by sparse vegetal cover. Most raindrops are impeded by leaves and trunks of the vegetal cover, in a process known as **interception.** Interception substantially reduces not only the erosive potential of raindrop strike but also the volume of water reaching the surface. Interception losses are quite variable because they depend on numerous hydrometeorological factors, vegetation type, land use, and seasonality. In addition, the loss is dependent on storm duration, being initially high and decreasing as the storm continues. During long storms, the vegetation may become saturated and all additional rainfall is passed on to the surface. Nonetheless, interception typically removes 10 to 20 percent of precipitation where grasses and crops are the dominant vegetation and up to 50 percent under a forest canopy (Selby 1982). Rainwater that does reach

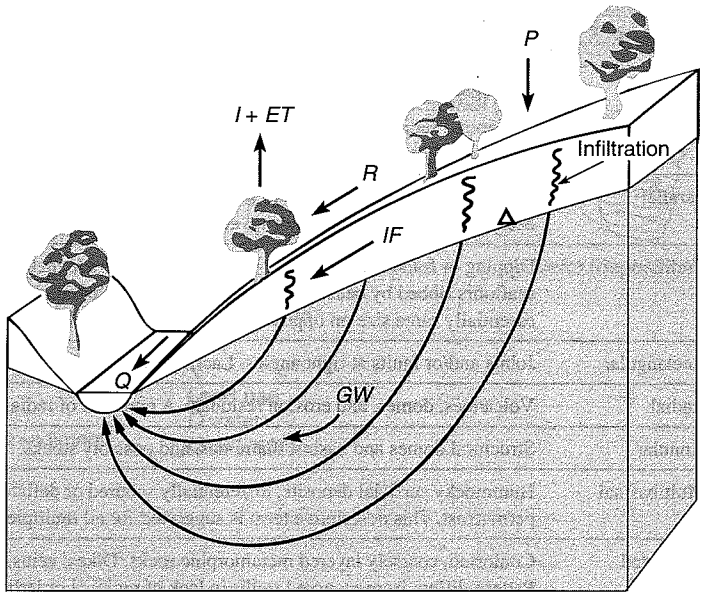

Figure 5.3
Slope hydrologic cycle. Some of the precipitation (*P*) is intercepted by vegetation (*I*) or lost by evapotranspiration (*ET*). Upon reaching the ground surface, it becomes part of stream discharge (*Q*) by direct runoff (*R*), interflow (*IF*), or groundwater flow (*GW*) after it reaches the water table (Δ).

the ground may still be prevented from contributing to streamflow by vegetation because some of it is consumed and lost by **evapotranspiration.**

Infiltration

Water on the ground surface may follow different routes to a stream channel. Water flowing into a channel in direct response to a precipitation event is called **storm runoff** or **direct runoff,** whereas the process of water entering the soil is considered **infiltration.** In 1933 Horton suggested that the rate of infiltration into soil on a sloping surface actually governs the amount of storm runoff generated by rainwater. This infiltration theory of runoff can be described as follows. Imagine a hypothetical slope with a surficial mantle of regolith formed by weathering and mass wasting processes. As precipitation falls on the slope surface, water is absorbed into the ground at a rate called the **infiltration capacity.** Infiltration capacity, typically measured in mm/hr is a function of regolith or soil thickness, soil texture, soil structure, vegetation, and the antecedent condition of the soil moisture (which depends on the recent history of precipitation). The rate of infiltration depends primarily on the interaction between three processes: (1) absorption or entry of water into the soil, (2) storage of water in the pore spaces, and (3) transmission of water downward through the soil. Infiltration rates are generally maximized when slopes are gentle with permeable soils and when rainfall intensity is low.

Recent studies of basins within the same climatic setting have shown that runoff processes, and thereby the surface hydrologic parameters such as discharge of water and sediment discharge by channels, are significantly impacted by variations in basin lithology. Kelson and Wells (1989) observed that unit runoff was consistently higher from basins underlain by resistant crystalline rocks than from neighboring watersheds underlain by less resistant sedimentary rocks in the mountains of northern New Mexico. Differences in regolith production from weathering of the parent lithology and from earlier geomorphic activity (i.e., glaciation) contributed to differences in the timing of water inputs into the basin, variations in subsurface slope, infiltration capacity, and the sediment yield and erosive power of the basin streams. Sala (1988), in a comparative study of watersheds underlain by slate and crystalline rocks in Spain, found that regolith variations attributed to the lithology not only resulted in notable differences in runoff but also produced general differences in process dominance on basin hill-slopes. Slate watersheds generated large amounts of coarse debris and were dominated by creep, leading to high erosion rates. On the other hand, crystalline basins were characterized by well-integrated runoff systems with perennial flow due to thicker regolith composed of grus. Therefore, infiltration capacity varies spatially on a large scale with regional geology, but may also change locally (even along the same slope) if the controlling factors vary.

Infiltration capacity normally changes at a site during any precipitation event (fig. 5.4). It usually starts with a high value that decreases rapidly during the first few hours of the storm and then more slowly as rainfall continues, until it finally attains a reasonably constant minimum value. Typically, the ultimate infiltration rate is established by a limiting subsurface horizon with a low water transmission rate, such as a zone of textural B horizon, caliche, or the bedrock surface. The infiltration capacity changes because surface conditions change during a storm, especially as aggregated soil clumps are broken apart into smaller particles which clog some of the pores. In the time interval between rains, the infiltration

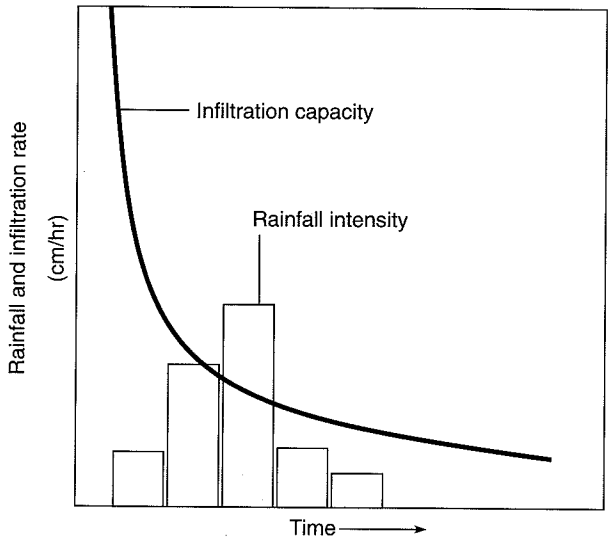

Figure 5.4
Infiltration capacity and rainfall intensity plotted against time. Infiltration capacity decreases with duration of storm. Runoff occurs only when rainfall intensity is greater than infiltration capacity.

capacity rises again as the surface dries and reestablishes its aggregated structure, and storage space within the soil increases again as soil water gradually drains downward. The frequency of rainfall, expressed as time between successive rains, can also become a significant factor affecting infiltration. Rains of relatively minor intensity may trigger disastrous floods if the infiltration capacity does not have enough time to recover between storms.

In Horton's model, as long as the infiltration capacity exceeds the rate at which rainfall strikes the surface (known as *rainfall intensity*), all incoming water will be infiltrated and none will run off. However, in those periods when rainfall intensity exceeds the infiltration capacity, runoff will occur as water moving down the slope surface; this runoff is known as **Hortonian overland flow.** Hortonian overland flow has been considered to be the primary determinant of peak flow and total direct runoff in a stream channel from a storm because its flow velocity generally ranges between 10 and 500 m/hr (Dunne 1978). The basic assumption here is that all infiltrated water is delayed greatly in its procession to the stream channels because it must percolate downward to the groundwater table and then move toward the stream by comparably slow groundwater flow velocities (see fig. 5.3). Overland flow, which occurs as broad shallow sheets or in linear depressions called *rills* is uncommon, however, except in sparsely vegetated semiarid and arid regions. Hortonian flow is virtually nonexistent in humid-temperate regions characterized by dense vegetation and thick soils (Kirkby and Chorley 1967; Dunne and Black 1970a, 1970b).

In light of the above, we must ask the logical question as to where the water comes from to produce the rapid peak flows observed in small basins of humid regions if all rainwater reaching the surface is subject to infiltration.

Subsurface Stormflow and Saturated Overland Flow

A major flaw in Horton's original model was the belief that infiltrated water moved directly downward under the influence of gravity. Research subsequent to Horton's analyses has clearly demonstrated a variety of flow within the unsaturated zone, due to the anisotropic character of regolith in most areas with respect to its ability to transmit water. Thus, significant lateral and subhorizontal flow can occur in some areas. Infiltrating water moves downward from the surface as a wetting front to the water table. In doing so, the front often encounters a soil horizon or other zone of low permeability that not only limits infiltration capacity but also tends to divert water downslope (often laterally) along its surface. This occurs because a local saturated condition develops above the low permeability zone, and lateral flow is initiated parallel to the barrier. This type of movement, called **throughflow** or **interflow** (Kirkby and Chorley 1967), can occur above the water table and permits water to take a more direct path to the stream channel than normal groundwater does. Throughflow is probably most common in the more permeable A horizon.

Where no barrier exists, infiltrated water will reach the water table and elevate its position. The water table rises rapidly adjacent to the channel, where antecedent soil moisture is greatest, and slowly in the upper-slope zone. As a result, the water table steepens immediately next to the channel and generates accelerated groundwater flow in that area. The combination of throughflow and accelerated groundwater movement is called **subsurface stormflow.** It was first recognized by Hursh (1936; Hursh and Brater 1941), but the significance of the concept was not fully realized until much later.

Subsurface stormflow from the lower parts of slopes may actually produce runoff in the form of bank seepage early in a storm. Therefore, it is possible for some of the subsurface stormflow to contribute to peak discharge. In other situations, storm runoff is generated from the movement of subsurface water through **macropores,** which are linear openings, having a much greater permeability than the surrounding regolith (Mosley 1979; Bevan and Germann 1982). Macropores can originate along root channels by **piping** (flow concentration and erosion along the rigid root) or in voids left by decayed roots, burrows, and other cavities made by plants and animals. Flow through such pipes can be rapid and turbulent, accounting for as much as one-fifth of the

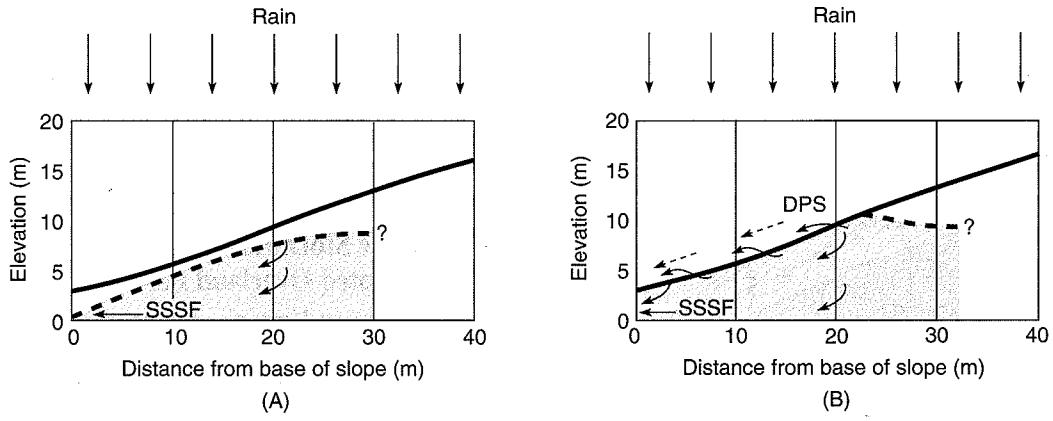

Figure 5.5
Runoff and interflow in a steep, well-drained Vermont hillslope. (A) Early in a storm the saturated zone (shaded) yields a small amount of subsurface stormflow (SSSF). (B) Late in the storm the water table rises to the surface as return flow (RF). Precipitation on the saturated area (DPS) adds to the return flow.
(Dunne and Leopold 1978)

annual contribution to runoff from hillslopes (Roberge and Plamondon 1987). Although some water may enter channels rapidly by these processes, most studies show subsurface flow to be a more important contributor to streamflow after the discharge peak, because measured velocities of subsurface flow range between 0.003 and 1.0 cm/hr (Dunne 1978), too slow to effectively contribute to most peak flows in small basins. This slow response requires yet another source of runoff to help explain the rapid production of peak flood flow. A field experimental study in a forested Appalachian watershed reported distinguishable inputs into surface runoff from throughflow sources (Hornberger et al. 1991). Significant contributions to storm runoff may occur where soil conductivity (with respect to its ability to transmit water) is high due to coarse texture and/or the presence of large macropores.

Detailed studies in Vermont (Ragan 1968; Dunne and Black 1970a, 1970b) showed that in many storms the level of the water table rises until it actually intersects the ground surface near the stream channel (fig. 5.5). In addition, zones of throughflow partially fed by laterally moving, infiltrated water may become saturated to the surface (Kirkby and Chorley 1967). In this situation some of the infiltrated water is returned once again to the surface and begins to flow downslope toward the channel; this flow is aptly called return flow. **Return flow** is obviously a form of overland flow, but its origin and location is distinctly different from Hortonian overland flow. The velocity of return flow is much greater than subsurface stormflow, attaining speeds of 3 to 15 cm/sec (Dunne 1978). In addition, direct precipitation on the saturated area marked by return flow or zones of saturated throughflow adds significant amounts of water to the volumes of direct runoff.

The combination of return flow and direct precipitation on saturated areas, called **saturation overland flow,** is now documented in many humid areas as the major contributor to direct runoff to stream channels. For example, Ragan (1968) estimated that on the average it supplied 55 to 62 percent of the total storm runoff in a small watershed near Burlington, Vermont, and was predominant in determining peak discharge. Subsurface storm flow then provided 36 to 43 percent of the total flow but exerted its greatest influence after the peak during the recessional phase of the runoff.

There are many sources of direct runoff other than Hortonian overland flow. Moreover, it is becoming apparent that the area of a watershed actually providing runoff during a storm is not temporally constant. This perception, known as the *variable source concept* or *partial area concept,* indicates that the area over which quick runoff occurs varies seasonally and during any given storm (fig. 5.6). This change is fundamentally controlled by topography, soil characteristics, antecedent moisture, and rainfall properties, and essentially means that there will be seasonal changes in the extent and location of channel networks contributing to surface flow (de Vries 1995). Areas with moderate to poorly drained soils, gentle slopes, and concave recessions along the valley walls are prone to have the greatest expansion of contributing areas during storms and on a seasonal basis.

Although the generalizations discussed above seem reasonable, they are based on a limited number of studies, and much more work is needed to refine the model (Selby 1982). Nonetheless, the observations about runoff generation have an important bearing on the geomorphic processes operating within a drainage basin, and further research in this field should be vigorously pursued (Freeze 1980).

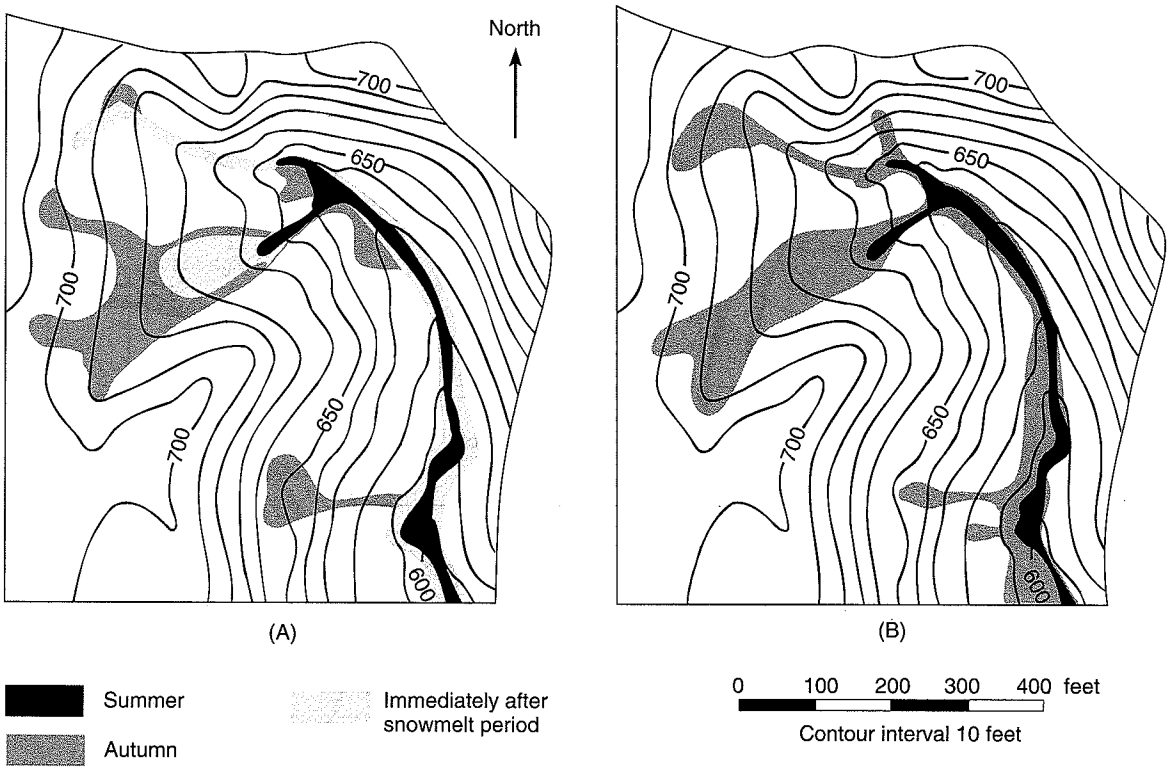

Figure 5.6
Variations in saturated areas on well-drained hillslopes near Danville, Vt. (A) Seasonal changes of prestorm saturated area. (B) Expansion of saturated area during a single 46 mm rainstorm. Solid black represents beginning of storm. Light shade represents saturated area at end of storm where water table has risen to the surface.
(Dunne and Leopold 1978)

The Stream Hydrograph and Response to Basin Characteristics

Hydrologists have always been concerned about how much runoff will issue from any precipitation event and how quickly the runoff will enter the stream channels. These factors determine if and when a flood will occur and what height the river will reach at peak flow. Figure 5.7 compartmentalizes the hydrologic processes that contribute to flood runoff in a stream channel. The response of the stream to a storm is depicted graphically as a **flood hydrograph** (or storm hydrograph), which shows the passage of flood flow volume, or *discharge,* with time (fig. 5.8). Discharge can be separated, using one of numerous separation techniques (see Chow 1964), into **direct runoff** and **base flow.** Runoff represents the sum of numerous types of overland flow, interflow, and stormflow, whereas base flow arises from contributions of groundwater spread out over longer periods of time. Whereas discharge may contain elements of both if measured shortly after a storm, base flow is the sole source of water sustaining river flow in dry periods between storms.

The maximum or peak flow usually develops soon after the precipitation ends, separating the hydrograph into two distinct segments, the *rising limb* and the *recession limb.* **Lag time** is the time between the center of mass of the rainfall and the center of mass of the runoff. The rising limb generally reflects the input from direct runoff; hence, the increase in discharge with time is relatively rapid. The recessional phase, however, is controlled more by the gradual depletion of water temporarily stored in the shallow subsurface system, and thus the decrease is less pronounced with time. This phenomenon normally results in an asymmetrical hydrograph, unlike the one shown in figure 5.8. In addition, the shape of the recessional limb is not influenced by the properties of the storm causing the increased discharge but is more closely related to the physical character of the basin.

Effect of Physical Basin Characteristics

The physical characteristics of a basin contribute to the magnitude of the flood peak. The shape of the flood hydrograph is influenced not only by the temporal and spatial distribution of the rainfall, but in large manner by the physical character of the drainage basin. The flood hydrograph represents the integrated effects of basin area, channel density and geometry (basin morphometry), soils, and land use and thus is the summation

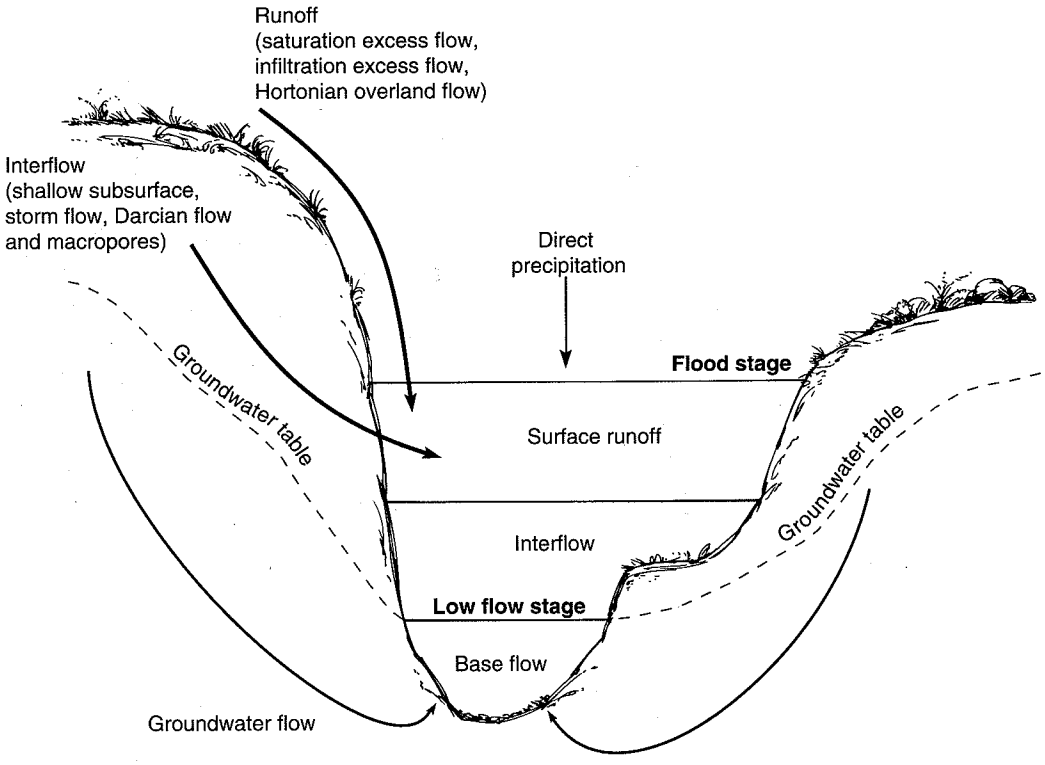

Figure 5.7
Schematic of stream channel showing major kinds of water contributions. Arrival of water from any given precipitation event is progressively delayed from runoff to interflow to groundwater flow.
(Based on Kochel 1992)

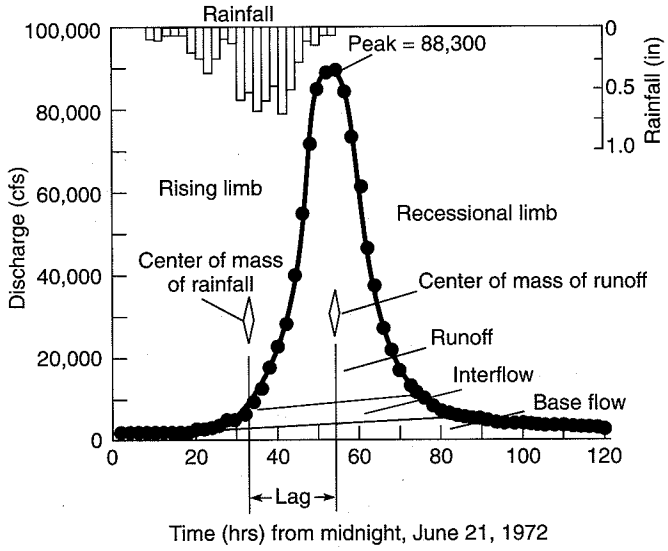

Figure 5.8
Flood hydrograph of the Hurricane Agnes flood of June 1972 on the Conestoga River at Lancaster, Pa. Although the curve is rather symmetrical, most hydrographs show significant skewness with a broader recessional limb reflecting interflow and groundwater inputs after a storm.

of the physical processing of precipitation from the divides to the site of measurement. Sophisticated models have been developed to predict how water is collected, stored, routed, and summed from all parts of a basin to achieve a final output hydrograph (for example, U.S. Army Corps Engineers 1985). If geology and topography are alike throughout an area, then rainfalls having similar properties should generate hydrographs with the same shape. On this premise, a *type* hydrograph for a basin, called a **unit hydrograph,** has been developed, in which the runoff volume is adjusted to the same unit value (i.e., one inch of rainfall spread evenly over the basin over one day). The unit hydrograph has been used as a connecting link in many studies attempting to relate basin morphometry to hydrology. By comparing the shapes of unit hydrographs from different basins, we can see the effects of differences in physical attributes of the basin.

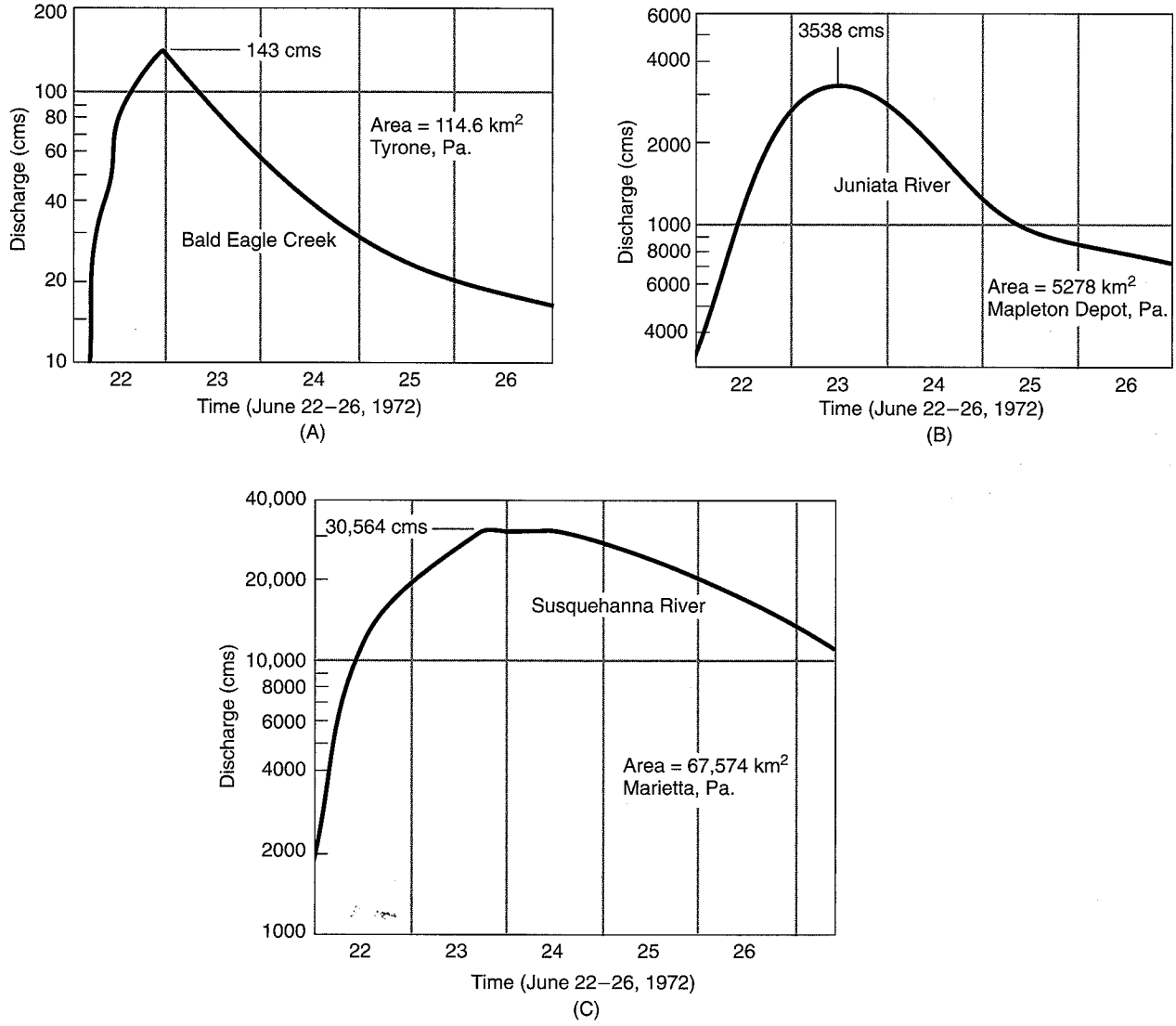

Figure 5.9
Progress of flood crests caused by Hurricane Agnes in the Susquehanna River basin, June 1972. Basins of increasing size: (A) Bald Eagle Creek; (B) Juniata River; (C) Susquehanna River.

Basin lag is the time needed for a unit mass of rain falling on the basin to be discharged through the measuring point (or basin outlet) as streamflow. Basin lag is normally estimated as the time interval between the centroid of rainfall and the centroid of the flood hydrograph (fig. 5.8) and is comprised of two distinct parts, the time involved in overland flow and the channel-transit time. Lag time for any basin is fairly consistent, with minor variations sometimes caused by the position and movement of the storm center relative to the gaging station. It seems intuitive that lag should increase with the size of the basin, but comparisons of similar-sized basins can show lag times up to three times as *sluggish* as basins with short lag times, which are referred to as *flashy* streams. Lag, therefore, is influenced by parameters other than drainage area alone, such as basin slope, the density of channels in the basin, and soils.

The time elements of basin hydrology can have a monumental influence on the magnitude of peak discharge during floods. Take, for example, the progression of flood crests recorded at several gaging stations in the Susquehanna River basin during the Hurricane Agnes flood in June 1972 (fig. 5.9). Most of the precipitation entered the basin during the period between June 19 and June 22. In the minor tributary Bald Eagle Creek, the flow peaked at 143 cms (5050 cfs) on the night of June 22, indicating a relatively quick response to the storm. In the larger Juniata River, the flood crested about 12 hours later with a considerably higher discharge value of 3538 cms (125,000 cfs). Far downstream on the main Susquehanna River, the flood peak did not occur until 12 hours after the Juniata peak, when discharge rose to 30,564 cms (1,080,000 cfs). Discharge peaked later on the main stream, and at a significantly higher magnitude than in the tributaries.

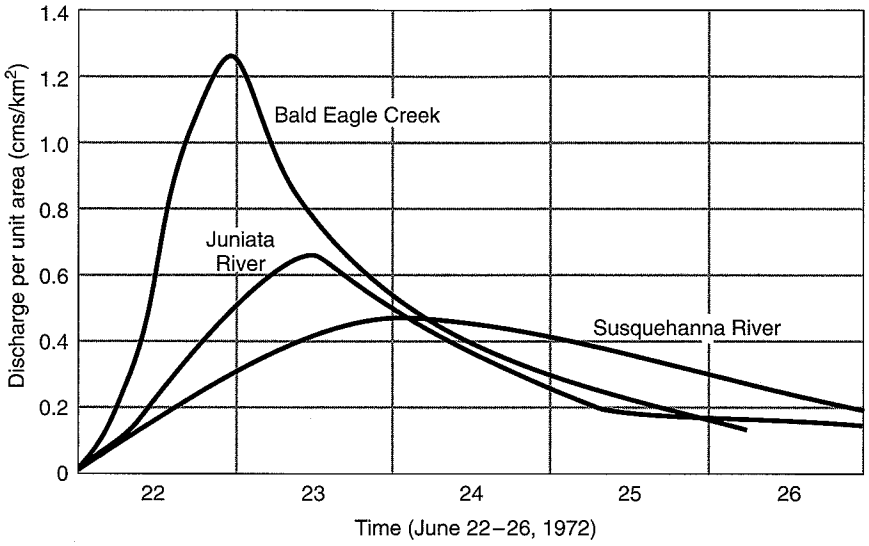

Figure 5.10
Discharge per unit area during flood caused by Hurricane Agnes in the Susquehanna River basin, June 1972. Note that the main river has considerably less discharge/area than tributaries. Main stem also peaks later and discharges floodwater over a longer time period, showing the effect of storing water on floodplains.

Lag time and peak discharge are positively correlated with basin size. However, simple expansion in basin size cannot fully explain the observed flow characteristics during a flood. Using data from figure 5.9 and replotting the peak discharge as Q/km^2, figure 5.10 reveals the interesting hydrologic property that discharge per unit area is much higher for the smallest tributary than for the massive basin of the main stem. Figure 5.11 shows how a similar relationship between basin area and discharge can be useful as a guide for anticipating the maximum flow likely for a basin of a given size. Had the increase in discharge during the 1972 Susquehanna flood been only a function of increased basin area, the peak flow at the Marietta station should have been a simple product of the Q/km^2 value of Bald Eagle Creek times the drainage area above Marietta, or 1.25 cms/km^2 × 67,574 km^2 = 84,468 cms (2,978,454 cfs), but this is almost three times the actual measured value. Somewhere within the basin, a built-in flood control mechanism exists that not only holds down the magnitude of the peak Q but simultaneously maintains abnormally high flow over a longer period of time. Most of this ability to lower peak flow can be attributed to the storage of water on floodplains and riverine wetlands. Floodplains store or retard large volumes of water until the flood crest passes a given channel locality. Additionally, differences in flood-crest travel time on the numerous tributaries in the basin and vagaries introduced by variable sources of runoff may help retard the downstream peak flow. Thus, a portion of runoff never contributes to the increasing of peak flow downstream but shows up in the record after the crest has passed as the extended part of the recessional limb of the flood hydrograph.

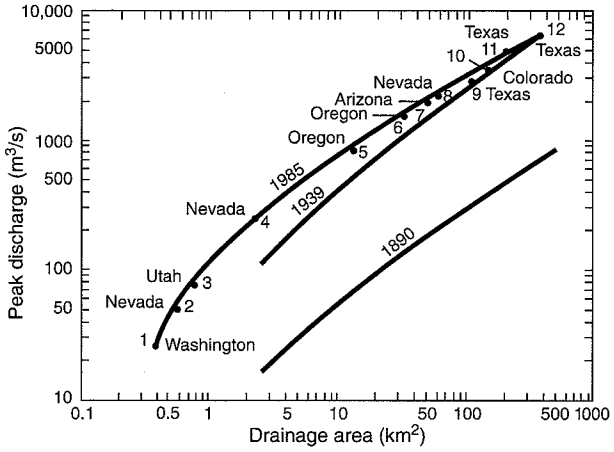

Figure 5.11
Peak discharge per unit from the largest flash floods in U.S. history. Note how the relationship indicates an increase in discharge coincident with development and land use alterations over the past 100 years.
(From Costa 1987)

Initiation of Channels and the Drainage Network

In the Horton model, when rainfall intensity exceeds the infiltration capacity, overland flow occurs and only then does erosion become possible (see fig. 5.4). For a stream channel to develop, the erosive force (F) of the overland flow must surpass the resistance (R) of the surface being eroded. According to Horton (1945), as overland flow begins to traverse the slope, the force it exerts on a soil particle depends on the slope angle, the depth of water, and the specific weight of the water. Actually, F represents a shear stress exerted parallel to the surface by the

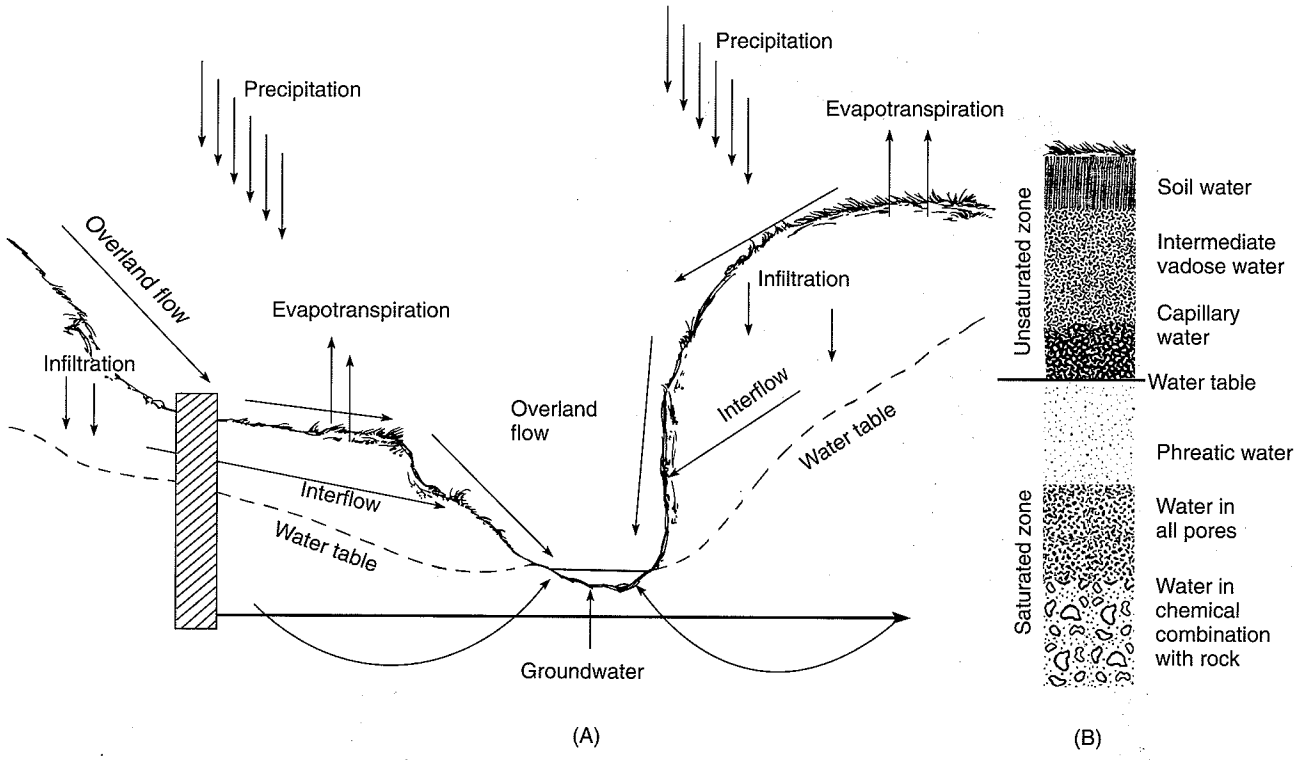

Figure 5.26
Surface and shallow subsurface hydrology of a watershed. (A) Schematic of basin showing directions and relative water movements measured in discharge (volume per time). (B) The groundwater profile as it would appear in homogenous material in the vertical slice on the left.

able to delineate blind subsurface faults and faults using abnormalities of basin networks in the Philippine Islands.

BASIN HYDROLOGY

For planning purposes, estimates are needed of how much water exists in a drainage basin and whether it is available for use. Hydrologists usually employ a concept known as the **water balance** or **hydrologic budget** to make such estimates. The water balance simply refers to the balance that must exist between all water entering the basin (input), all water leaving the basin (output), and any changes in the amount of water being stored.

Figure 5.26 illustrates the hydrologic cycle with respect to a drainage basin. The major inputs are rainfall and snow, and the major outputs are evapotranspiration and streamflow. Water is stored in lakes, soil moisture, and groundwater, and changes in these values actually represent losses or gains of available water. Although the basin cannot actually be divorced from the global hydrologic system, we can view the basin hydrologic budget simplistically by the following equation:

$$\Delta S = I_P - O_E - O_T - O_R$$

A change in storage, measured as recharge to the groundwater system (ΔS), is equal to the difference between input as infiltration from precipitation (I_P) and losses or outputs from evaporation (O_E), transpiration (O_T), and runoff (O_R). Although runoff provides the predominant connection between our basin and the global hydrologic system, some groundwater may exit the basin by regional subsurface flow pathways. For example, a positive change in groundwater storage indicates that the underground reservoir is being recharged, but in the budget it represents a loss because the availability of the water is being lowered. On the other hand, groundwater runoff (base flow) represents an input because water availability is increased as it is released from storage.

Subsurface Water

The increased demand for water that has accompanied population growth, industrial expansion, and extended irrigation in the United States has brought with it a marked increase in the utilization of groundwater. Groundwater as a resource is highly sought after because it typically maintains chemical and physical characteristics that fluctuate far less radically than surface water supplies. For example, groundwater maintains a constant year-round temperature, a more constant chemical composition year-round, and is less affected by periodic droughts than surface reservoirs. The volume of water contained in fractures and pores in Earth's underground reservoir is

enormous; it is estimated at almost 8 million km^3 in the outer 5 km of the crust (Todd 1970). Unfortunately, this vast resource is not evenly distributed. Some regions are blessed with abundant groundwater whereas others are seriously deficient. Ironically, many of the most rapidly expanding areas of the United States are in regions with low reserves of surface and groundwater. The lack of available water, coupled with the growing demand and ever-present threat of contamination, poses a major challenge to geologists and requires that we continue to expand our knowledge concerning the distribution, movement, and utilization of groundwater. For example, some regions possess groundwater with exceptionally high natural concentrations of dissolved minerals, whereas others are plagued by anthropogenic contaminants. Groundwater geology, or **hydrogeology,** has evolved into a separate discipline in itself; however, because it is an important part of basin hydrology, we will briefly examine how the groundwater system works.

The Groundwater Profile Groundwater in porous and permeable rocks or unconsolidated debris usually has a rather distinct distribution that can be visualized as a vertical zonation known as the *groundwater profile* (fig. 5.26B). The *unsaturated zone* above the water table is variable in water content within its pores and fractures. Air occurring in pores that are only partly water-filled is physically connected to the atmosphere. Slugs of infiltrating water move vertically down, under the influence of gravity, through the unsaturated zone in response to episodic precipitation events at the surface. Flow paths include movement through the interstices of porous sediment and bedrock, flow through bedrock fractures, and accelerated flow along zones of increased permeability referred to as macropores such as root channels and burrows. Interruptions in the complete downward transfer of water through the unsaturated zone commonly result from water being held by surface tension or that which is extracted by plants during evapotranspiration.

The uppermost portion of the unsaturated zone is the *zone of soil moisture,* which experiences large fluctuations in water quantity and quality because of variations in infiltration, evapotranspiration, and atmospheric pressure. The *intermediate zone* below the soil moisture zone experiences downward flow toward the water table. This zone, commonly thick in semiarid regions, may be totally absent in many humid areas.

The base of the unsaturated zone is marked by a zone of variable thickness where all available pore space is saturated with water. This area of apparent saturation is known as the *capillary fringe.* Capillary action draws water upward through the pores from the zone of saturation and holds this water in tension. Even though this zone is saturated, water will not drain freely into a well placed within the capillary fringe because the hydrostatic pressure remains less than atmospheric pressure, as it does throughout the unsaturated zone. The thickness of the capillary fringe depends on pore diameter, its thickness being inversely proportional to the diameter of the pores.

All pore spaces below the capillary fringe are filled with water; hence this area is called the *saturated* or *phreatic zone.* Phreatic water will drain freely into a well because the hydrostatic pressure in this zone exceeds that of atmospheric pressure. The *water table* marks the level where the hydrostatic pressure is equal to atmospheric pressure and defines the upper boundary of the saturated zone. This zone extends downward until rocks become dense enough that small occurrences of interstitial water are no longer interconnected. The saturated zone may extend for tens of thousands of feet in sedimentary basins, being less extensive in crystalline rocks.

Movement of Groundwater Water in the saturated zone is not static but can move in any direction depending on the distribution of potential energy fields within the zone. Groundwater flow in the saturated zone is not solely regulated by gravity as it is in the unsaturated zone. Each unit volume of water contained in the saturated (phreatic) zone possesses a certain amount of potential energy, called its *potential* or *head.* The amount of potential varies from droplet to droplet, being dependent on the pressure of each drop and its elevation above some datum. When pressure and elevation are known, the potential for each unit volume of water can be calculated, and water particles having the same potential can be contoured along surfaces known as *equipotential surfaces* (fig. 5.27). Although some diffusion occurs, groundwater particles move along paths that are perpendicular to equipotential surfaces.

The movement of groundwater is a mechanical process whereby some of the initial potential energy of the water is lost to friction generated as the water moves. It follows that water moving from one point to another must have more potential energy at the beginning of the transport route than at the end. Thus, groundwater always moves according to the following rules: (1) it moves from zones of higher potential toward zones of lower potential, and (2) it flows perpendicular to the equipotential surfaces, at least in simple homogeneous and isotropic materials (Hubbert 1940).

The velocity and discharge of groundwater flow is directly proportional to the loss of potential (head) that occurs as water moves from one point to another (fig. 5.28). This concept was demonstrated in 1856 by H. Darcy in his famous experiments on flow through porous media. He also observed that flow velocity was inversely proportional to the length along the flow path. Darcy's experiments led to the fundamental law of groundwater flow, expressed as

$$V = K\frac{h_1 - h_2}{L}$$

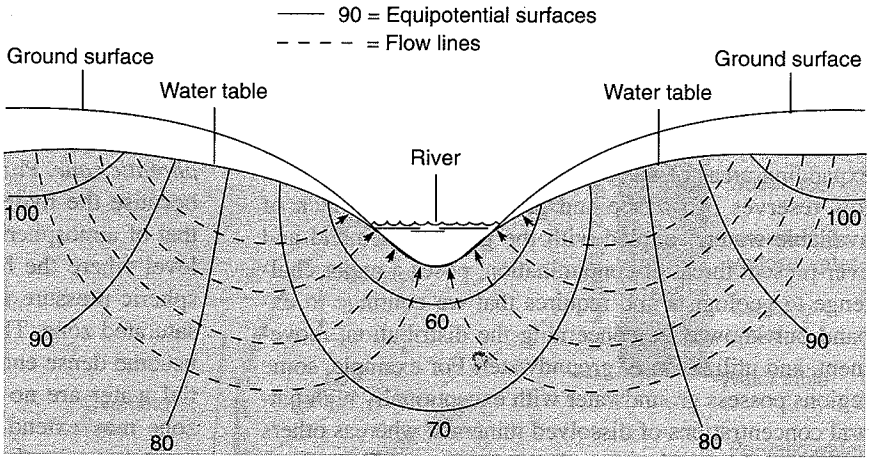

Figure 5.27
Movement of groundwater according to distribution of potential in the underground system. Water moves from high to low potential and perpendicular to the equipotential surfaces.

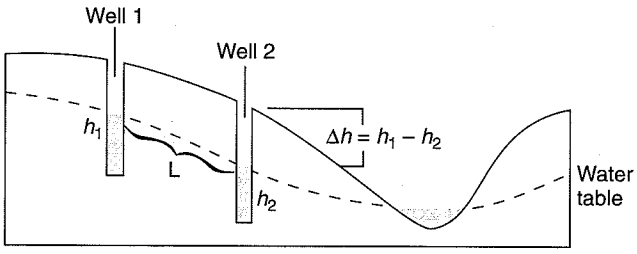

Figure 5.28
Water table and loss in head as water moves from well 1 to well 2 in unconfined aquifer.

where V is a volumetric flow rate similar to velocity, h is head, L is the distance between the two points of measurement (i.e., between monitoring wells), and K is a constant of proportionality representing the permeability of the medium, known as the *hydraulic conductivity.* In figure 5.28, the velocity of flow can be calculated from the difference in hydrostatic level (head) between two wells ($h_1 - h_2$) if the permeability of the material is known or can be estimated. Discharge can also be calculated by including the cross-sectional area of the aquifer to the equation so that

$$Q = K\,I\,A$$

where Q is discharge, A is the cross-sectional area of an aquifer perpendicular to flow ($w \times d$), and I, called the

$$\textit{hydraulic gradient}, \text{equals} \frac{h_1 - h_2}{L}.$$

Darcy's Law is applicable to groundwater flow through porous materials, but adjustments are often made to accommodate the effects of variable media and fluid properties on the actual values of K. More complex relationships must be used to estimate flow characteristics through fractures in relatively impermeable host materials.

The water table, at the top of the phreatic zone, is an important hydrologic feature (see fig. 5.26). Because hydrostatic pressure everywhere along the surface of the water table is equal to atmospheric pressure, the potential of the water table is equal to atmospheric pressure. The potential of water there is completely a function of elevation, and water at this surface will always move from higher to lower elevations. This partially explains why the water table is generally a mirror image of surface topography. Whereas surface water and groundwater systems are physically connected, the levels of rivers, lakes, swamps, and other wetlands are merely surface extensions of the underground water table (see fig. 5.27).

Aquifers, Wells, and Groundwater Utilization Problems *Aquifers* are lithologic bodies that store, transmit, and yield water in economic amounts. The most common aquifer is called an *unconfined aquifer* because it is open to the atmosphere and its hydrostatic level (shown by the level at which water will stand in a well) is within the water-bearing unit itself. The hydrostatic level in an unconfined aquifer is the water table. In some other aquifers the water is held in a porous and permeable unit that is not connected vertically to the atmosphere but instead is overlain and underlain by less permeable layers called confining layers (or aquitards). Water in these *confined aquifers* (fig. 5.29) will rise above the top of the aquifer when it is penetrated by a well or open hole. The level to which water will rise is called the *potentiometric surface.* The height of the potentiometric surface above the aquifer depends on the difference in potential at the point where precipitation or infiltration enters the aquifer, called the recharge zone, and the position of the screen at the base of the well or hole (fig. 5.29). If the potentiometric level is above the elevation of the ground, surface water will flow freely out of the well without pumping as *artesian flow.*

The development of an aquifer for water supply requires wells; the larger the demand, the larger and more numerous the wells. As a well is pumped, the hydrostatic level (water table or potentiometric surface) sur-

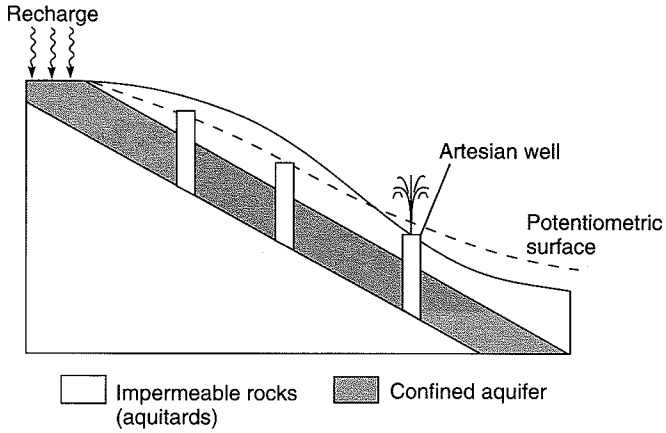

Figure 5.29
Confined aquifer and potentiometric surface.

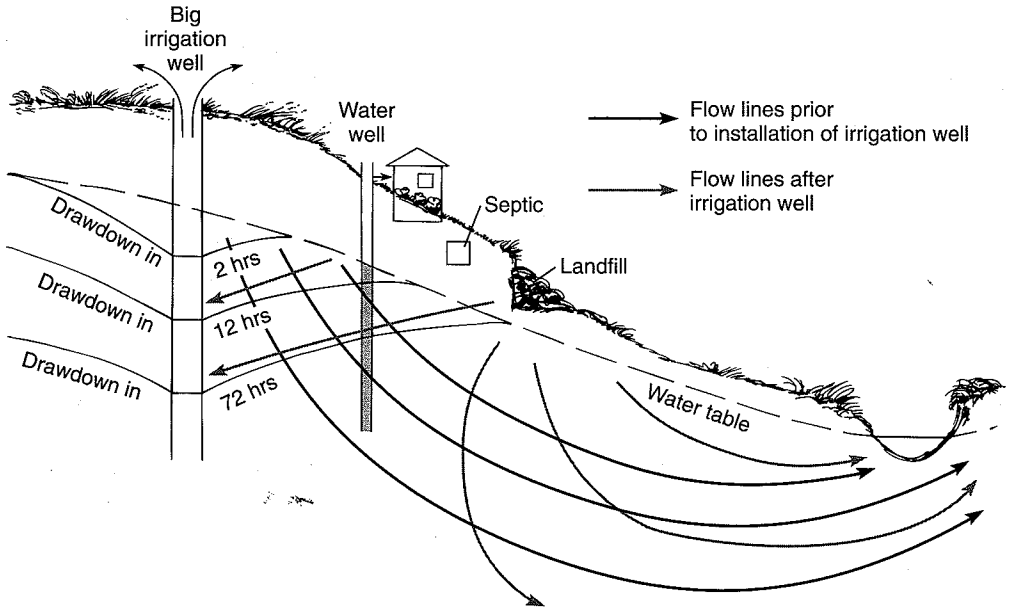

Figure 5.30
Development of cone of depression drawing down the water table due to the pumping of a major irrigation well. The cone of depression can alter groundwater flow patterns significantly as indicated here where the leachate from a landfill, which normally would move to the right, would now flow toward the water supply well for the home. This example assumes a simple homogenous system.

rounding the well declines and forms an inverted cone known as the *cone of depression* (fig. 5.30). The cone develops because the release of water (or of pressure in a confined aquifer) is greatest near the well. This causes pronounced lowering of the water table or potentiometric surface, called *drawdown,* adjacent to the well. The effect of pumping decreases away from the well, so drawdown is less toward the perimeter of the cone. In the initial phase of pumping, the rate of drawdown is normally high, but as pumping continues the rate gradually decreases until the cone attains a nearly constant form. The dimensions of the quasi-equilibrium cone depend on the rate at which the well is pumped and the hydrologic properties of the aquifer.

Utilizing groundwater can cause a number of environmental problems if the system is not studied carefully before development. For example, excessive drawdown can occur locally if wells are placed too close to one another and the radius of influence (the maximum diameter of the cone of depression) of adjacent wells overlap. This produces abnormally high drawdown in the zone of overlap because the drawdowns from all interfering wells are cumulative at any point. On a regional scale, most problems arise when more water is pumped from the aquifer over a period of years than is returned to the aquifer by natural or artificial recharge, a practice known as *overdraft.* In such a case the aquifer is actually being mined of its water, and on a long-term basis the

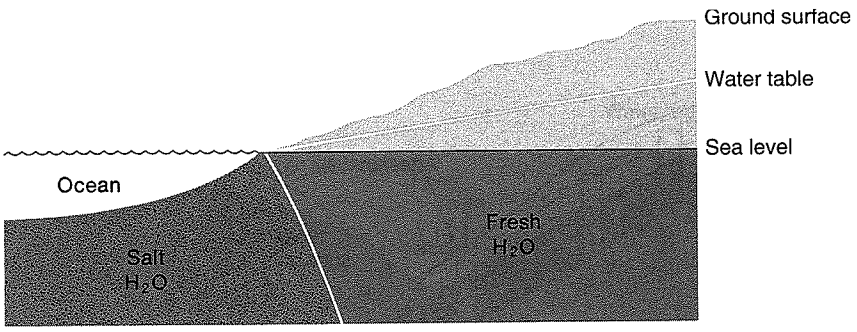

Figure 5.31
Relationship of salty and fresh groundwater in an aquifer of a coastal region. Lowering of water table by overdraft requires a 40-fold rise in the boundary between the fresh and salt water and increases the possibility of pollution of the aquifer by salt water.

normal hydrostatic level may be drastically lowered. The socioeconomic importance of these issues is well illustrated by an article in *National Geographic* (Zwingle 1993) that treats the concerns over depletion of groundwater in the major hydrostratigraphic unit of the U.S. High Plains region, the Ogallala Aquifer.

The effects of continued overdraft vary, but two types of responses will demonstrate the problems that can result from the misuse of the groundwater system. First, in confined aquifers, the drawdown of the potentiometric surface reflects the decrease of pressure within the aquifer. Because the pressure is lowered, water from the overlying confining layer seeps downward into the aquifer. As the confining layer drains, the normal load exerted by the weight of the overlying rocks compacts the confining layer and decreases its thickness. Ultimately, the process culminates in measurable subsidence of the ground surface. Some areas, such as Mexico City, Las Vegas, the Central Valley of California, and the Houston-Galveston area, have experienced 1 to 5 meters of overdraft subsidence, creating a variety of annoying and hazardous conditions such as cracking of buildings, strain on buried pipelines, highway subsidence, and destruction of well casings.

A second major effect of overdraft usually occurs in coastal regions where an aquifer is physically connected to the ocean. There, two fluids (ocean water and fresh water) having different densities are separated by a sharp boundary, as shown in figure 5.31. The location of the interface depends on the hydrodynamic balance between fresh water (density = 1.00 g/cm^3) and salt water (density = 1.025 g/cm^3). In general, the depth below sea level to the saltwater boundary is about 40 times the height of the water table above sea level. In such a situation, continued overdraft can cause pollution of the aquifer because minor lowering of the water table necessitates a much greater rise of the saltwater-freshwater interface, a phenomenon known as *saltwater intrusion.* For example, a 2-meter drawdown of the water table requires a concomitant 80-meter rise of the salt water, and any well extending to a depth greater than the new interface level will be polluted with nonpotable water. Calvache and Pulidd-Bosch (1991), using a numerical modeling approach, eloquently demonstrated how expanding groundwater withdrawal is responsible for the gradual encroachment of saline water into important regional aquifers in coastal Spain.

Many cities along the coasts of California, Texas, Florida, New York, and New Jersey have been affected by saltwater intrusion. This phenomenon, however, can occur wherever two fluids of different density exist within the same aquifer. For example, the water supply of Las Vegas, Nevada, is in jeopardy from pollution by high-magnesium groundwater located about 24 km south of the city. The intrusion is a response to the large overdraft from the aquifer beneath Las Vegas.

Linkages between groundwater and surface water systems have been the focus of many studies since the late 1970s. These have highlighted interactions related to channel initiation (Dunne 1990; Kochel et al. 1985), particle entrainment, floodplain aquifers and river-stage fluctuations (e.g., Sophocleous 1991), and the effects of shallow groundwater circulation on soil development and chemistry and of soil properties on groundwater (e.g., Richardson et al. 1992). In light of our ever-increasing concern about the environment, increased knowledge of the interactions between subsurface and surface hydrologic systems is becoming very important.

Surface Water

The major export from drainage basins to the global hydrologic system occurs as stream discharge. The volume of water passing a given channel cross-section during a specific time interval, is expressed as

$$Q = wdv = Av$$

where Q is discharge in m^3/s (cms) or ft^3/s (cfs), w is width, d is depth, A is area (wd), and v is velocity. Measurement of discharge is relatively simple by dividing the channel cross-section into segments of even width (fig. 5.32A). Depth and velocity are measured in each segment, and then total discharge is computed by summing the discharges of all of the sections across the channel. The most difficult measurement to obtain is velocity. Velocity varies with depth in open channels (fig. 5.32C), thus surface velocity is not very representative of the mean velocity. Average velocity is obtained

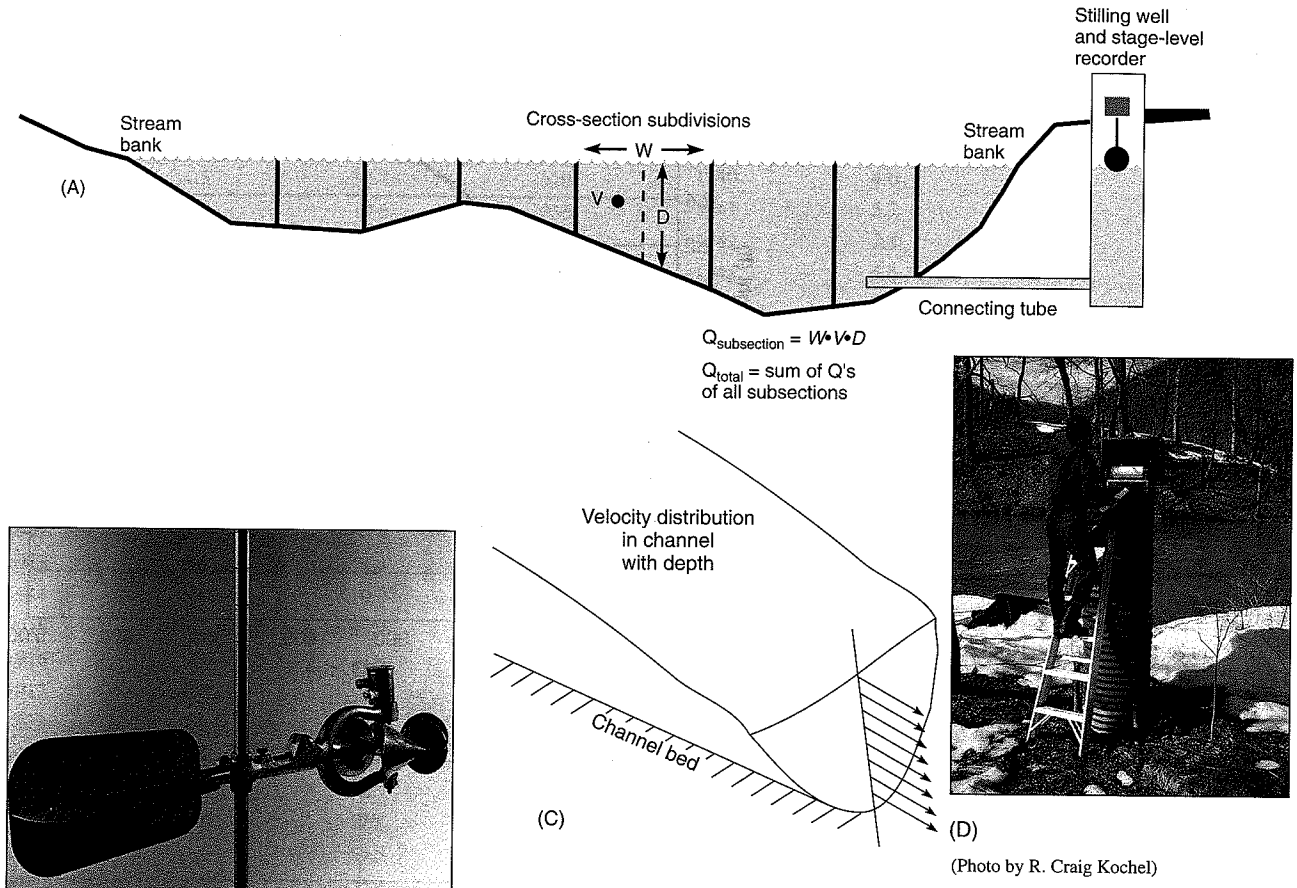

Figure 5.32
Stream discharge gaging station. (A) Channel cross-section subdivided into small compartments for discharge measurement in each. (B) Price current meter for measuring velocity. (C) Vertical profile of velocity in the channel. Average velocity can be measured just below half the depth. (D) Stream gaging station on Antes Creek, Pa. A rotating drum chart recorder is positioned at the top of a stilling well to monitor stage changes in the creek. The well is connected with the creek via lateral pipes below the floodplain.

with a current meter (fig. 5.32B) adjusted to measure the flow rate just below the halfway mark on the depth in each channel subsection.

To be of any scientific value, discharge must be measured repeatedly at the same locality; this gives hydrologists a better understanding of how flow varies with time. In the United States these sampling localities, or *gaging stations,* have been in operation at some sites since the late 1800s. Thus, a wealth of flow data for a large number of streams is available from the U.S. Geological Survey and numerous state water surveys. Common measurement frequencies vary from continuous recording to intervals of one hour. The average of these data are published annually as *mean daily discharge.* The *mean annual discharge* is the average of the daily values over the entire period of record, assuming that the station has been maintained for longer than one year.

Actually, discharge is not frequently measured by the procedure described above because it is very time-consuming. Instead, discharge is estimated from a *rating curve* (fig. 5.33), or *rating table,* which relates a range of discharge values to the elevation of the river above some datum, called the *river stage* or *gage height.* Once the rating curve for a specific station has been constructed from a series of actual discharge measurements (the data points on fig. 5.33), only the gage height must be observed directly to be able to predict discharge.

Flood Frequency Geomorphologists are interested in the frequency and magnitude of flow events because each has an important bearing on how basins and channels evolve and function. Mayer and Nash (1987) compiled a collection of papers focusing on the geomorphic effects and frequency of catastrophic floods. The

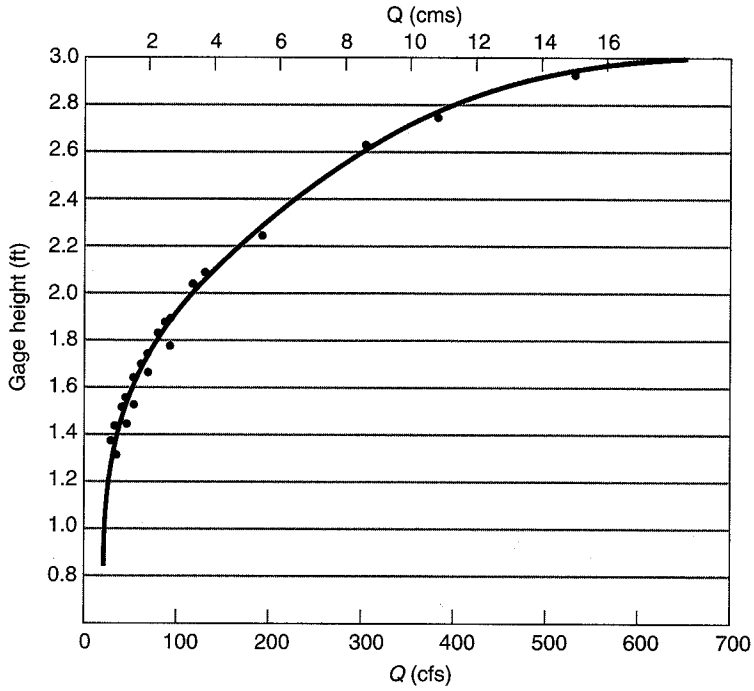

Figure 5.33
Rating curve for low flow. Rock Creek near Red Lodge, Mont.

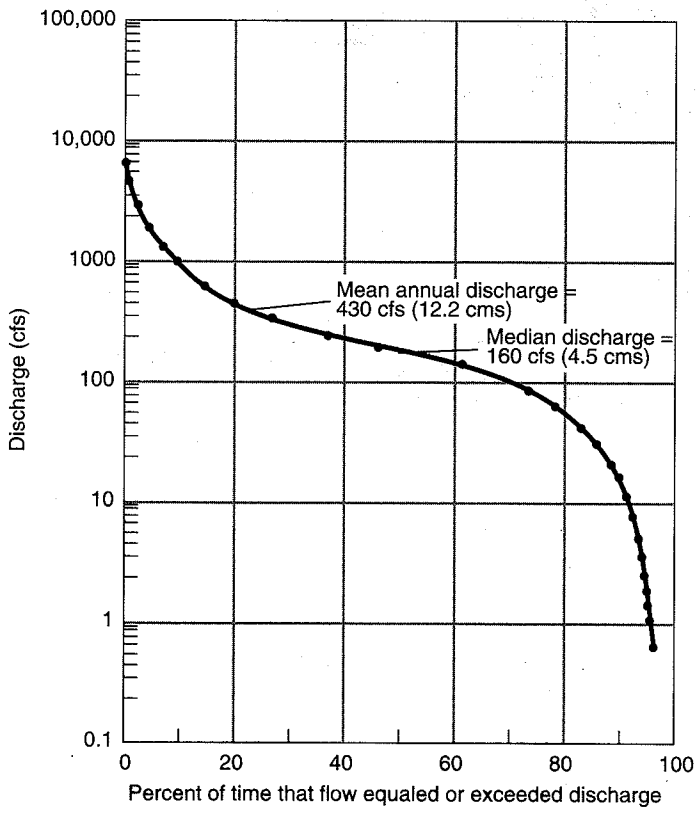

Figure 5.34
Flow duration curve for the Powder River near Arvada, Wyo., 1917–1950.
(Leopold and Maddock 1953)

frequency of a given discharge is graphed as a **flow duration curve** (fig. 5.34), which relates any discharge value to the percentage of time that it is equaled or exceeded. At any station, then, the lowest daily discharge in the period of record will be equaled or exceeded 100 percent of the time. The largest flow will be equaled or exceeded only once out of the entire number of days in the sample, giving it a percentage value slightly greater than zero.

The most common approach to finding the frequency-magnitude relationship (especially for floodplain planning) is to consider only the peak discharge during

TABLE 5.5 Annual Discharge Extremes and Averages for the Pecos River near Langtry, Texas, 1900–1977.

Year	Discharge (m3/s)			Year	Discharge (m3/s)		
	Minimum	Average	Maximum		Minimum	Average	Maximum
1900	7.3	—	2991	1939	3.9	8.1	162
1901	4.5	17.8	310	1940	4.6	8.8	157
1902	5.8	19.6	936	1941	5.7	51.4	523
1903	5.0	12.9	363	1942	7.4	21.8	264
1904	3.0	13.8	2013	1943	5.4	9.9	313
1905	14.2	40.8	1314	1944	4.4	8.1	250
1906	11.6	27.4	2516	1945	3.9	9.9	774
1907	5.0	12.9	327	1946	4.2	10.3	1817
1908	5.9	20.4	1901	1947	4.2	7.2	171
1909	4.2	10.1	727	1948	3.1	6.4	1434
1910	4.3	10.2	2851	1949	4.0	10.9	2753
1911	5.3	11.6	755	1950	2.8	7.2	1255
1912	3.4	6.4	512	1951	2.6	5.1	229
1913	3.8	15.4	1761	1952	2.3	3.9	100
1914	6.4	10.9	1873	1953	2.0	4.5	414
1915	10.2	32.9	1453	1954	3.0	78.3	27,392
1916	5.7	14.9	2711	1955	2.8	8.0	758
1917	4.1	8.3	176	1956	2.1	4.4	208
1918	2.9	6.1	1448	1957	3.3	15.1	1073
1919	3.5	30.8	243	1958	3.6	10.4	1075
1920	6.3	20.9	1219	1959	3.9	11.3	1328
1921	7.4	17.8	517	1960	2.9	5.7	134
1922	6.2	15.5	2152	1961	2.4	6.6	411
1923	4.2	6.9	358	1962	1.7	5.3	503
1924	3.6	10.0	1816	1963	2.2	4.1	88
1925	3.8	14.5	1705	1964	1.8	12.3	1037
1926	5.0	20.5	553	1965	2.9	6.5	436
1927	3.2	10.0	408	1966	2.9	7.4	433
1928	3.9	11.4	464	1967	2.6	—	60
1929	3.8	8.9	176	1968	2.6	5.0	626
1930	2.7	6.1	785	1969	2.3	5.5	172
1931	5.1	10.3	240	1970	1.7	3.7	62
1932	5.3	32.0	324	1971	2.0	13.6	2490
1933	6.7	11.9	126	1972	3.3	5.6	123
1934	3.8	6.8	229	1973	2.4	4.4	93
1935	3.6	4.4	2359	1974	1.6	41.9	16,128
1936	4.9	11.4	559	1975	6.0	9.3	274
1937	5.0	10.2	78	1976	3.9	10.8	1660
1938	5.3	12.1	881	1977	4.5	6.8	170

Source: Data from International Boundary and Water Commission.

each year (*annual series*) or only the discharges above some predetermined censoring value (*partial duration series*). The statistical samples in these time series approaches are much smaller than in the analyses utilizing daily records; however, they are useful in studies of major flow events, provided the gaging station has a record of considerable length. The annual discharges shown in table 5.5 have been ranked according to the magnitude during the years of record displayed. The **flood recurrence interval** can be calculated from an annual series like this one using one of a number of formulas. The simplest plotting formula, the Weibull Method, calculates the recurrence interval by taking the average time between two floods of equal or greater magnitude:

$$R = \frac{n+1}{m}$$

where R is the recurrence interval in years, n is the number of discharge values (the number of years in an annual series), and m is the magnitude rank of a given

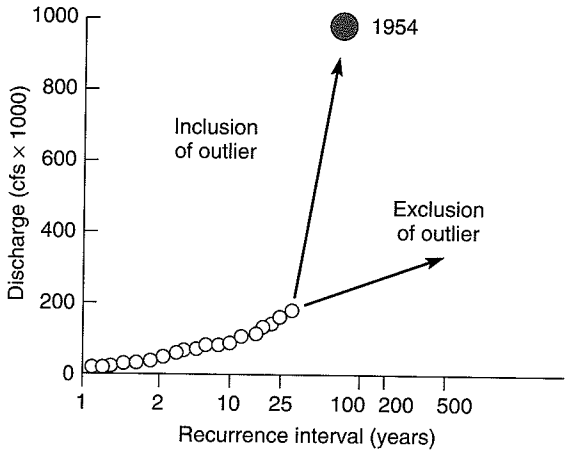

Figure 5.35
Flood frequency curve for the Pecos River near Langtry, Texas. Note the extreme outlier representing the 1954 flood and the problem for environmental planners of how to interpret this point.

flood. The results of this type of analysis are then plotted on probability graph paper to show the relationship of discharge to recurrence interval (fig. 5.35), and the curve is used by hydrologists to estimate the magnitude of a flood that can be expected *within a specified period of time.* U.S. governmental agencies have adopted another method called the Log Pearson Type III (U.S. Water Resources Council 1981), which utilizes three parameters from the annual flood series distribution—the mean, the standard deviation, and the skewness. There is little agreement among the experts as to which of the numerous analysis procedures works best (for a review and discussion of procedures for analyzing flood frequency see Dunne and Leopold 1978; Singh 1987; Klemes 1987; Kumar and Chandler 1987; Cunnane 1987).

The Pecos River flood frequency curve (fig. 5.35) shows that on the average the flow is expected to equal or exceed 2800 cms (100,000 cfs) once during a 25-year interval. Also from this curve, the 100-year flood would be estimated to have a discharge of about 27,400 cms (970,000 cfs) if the outlier is included. Bear in mind, however, that a flood recurrence interval estimate represents a probability statement and does not indicate that a flood of given size can only occur in time at regularly spaced intervals specified by its frequency. A river, unfortunately, does not understand statistical theory. Thus, there is no reason to believe that 25-year floods or 100-year floods will be distributed evenly over time. In the next 75 years, the Pecos River could experience three successive 25-year floods during the first 5 years, or there could be one now and several toward the end of the time period. Similarly, a flow equaling or exceeding the 25-year magnitude may fail to occur at all. The *probability* that a flow of a given magnitude will occur during any year is the reciprocal of the recurrence interval:

$$P = \frac{1}{R}$$

where P is the probability of flow being equaled or exceeded in any one year, and R is the recurrence interval. Thus, a 50-year flood has a 2 percent chance of occurring in any given year, and a 10-year flood has a 10 percent chance. Over a 100-year period, the 50-year flood has an 86 percent chance of occurring while the 10-year flood has virtually a 100 percent chance of occurrence, and so on. These probabilities are computed using the probability equation

$$q = 1 - \left(1 - \frac{1}{T}\right)^n$$

where q is the probability of a flood with a recurrence interval (T) occurring in the specified number of years (n) (Costa and Baker 1981). One should realize, however, that the chance of experiencing a flood of any specified recurrence interval is never zero; there is always some risk, and predicting the year in which it will happen is virtually impossible.

Even though it may be impossible to predict when a given flood will occur, magnitude-frequency analyses have considerable practical value in river management, especially for higher-frequency floods such as the 20-year (q_{20}), 10-year (q_{10}), or 5-year (q_5) floods. Using the annual series, the *mean annual flood,* which is the arithmetic mean of all the maximum yearly discharges in the sample, is the flow that should recur once every 2.33 years ($q_{2.33}$). In our Pecos River example the mean annual flood has a discharge of 790 cms (28,000 cfs) and plots at a recurrence interval of approximately 2.33 on the flood frequency curve (fig. 5.35).

Paleoflood Hydrology Perhaps the single most difficult problem faced by hydrologic planners is to estimate the magnitude of the maximum probable flood that can be expected to occur within any given basin. Such estimates usually require extension of the flood frequency curve far beyond the limits provided by historically measured flow events. In other cases, estimates are required for basins that have very short gaging records or lack any kind of historical record of flow events. This is very risky business because critical decisions about the type and cost of flood control and protection are based on these estimates. Most hydrologists agree that simple extension of statistical flood frequency relationships beyond about 1.5 times the period of historical record are invalid. In the United States, gaged observations rarely extend beyond 100 years, thus making assessments of flood magnitudes beyond the 100- to 150-year recur-

rence interval very uncertain. Standard hydrologic methods of estimating peak flood flows from basins lacking flood series data are similarly suspect.

Recently, geomorphologists have developed a suite of techniques that rely on the sedimentary and botanical record for information about floods that occurred along a given stream prior to direct observation or measurement. This approach is called *paleoflood hydrology* (Kochel and Baker 1982). Damage caused by floods to trees growing along the channel and floodplain can be used to establish the time of specific flood events, often down to a single year (Sigafoos 1964; Phipps 1985; Hupp 1988). Sometimes, the height of flood-induced damages on trees, such as corrasion scars, can be used to estimate a minimum flood stage (Yanosky 1982), thereby permitting estimates of paleoflood magnitude using standard indirect techniques to reconstruct flood flows (see Dalrymple 1960; Benson 1971). Costa (1983) reviews a number of flow regime-based techniques for reconstructing paleoflood depth and velocity that use the dimensions of flood-transported boulders in combination with the characteristics of channel cross-section and channel slope. A number of techniques focusing on analysis of Holocene floodplain stratigraphy have also been used to reconstruct paleoflood history. These techniques commonly interpret the stratigraphic sequence of floodplain sediments and the relationships between tributary fan sediments and mainstream sedimentation to bracket time intervals of major flow events (for example, see Costa 1978; Patton, Baker, and Kochel 1979; Blum and Valastro 1989).

One of the most successful and widely used stratigraphic approaches is based on the analysis of *slackwater deposits* (Kochel and Baker 1982; Kochel, Baker, and Patton 1982; Baker et al. 1983), which are relatively fine-grained sediments deposited in areas of backflow or flow separation from the main current. Application of the slackwater method works best in narrow bedrock reaches along streams where large stage increases result from small increases in discharge and where channel cross-sections are not subject to major change during floods. During high-flow conditions, water is backflooded into tributary mouths, shallow caves, eddies in areas of flow expansion, and in the lee of flow obstacles (fig. 5.36). These areas are characterized by relatively low-velocity conditions where sediment is deposited rapidly from suspension, leaving a record of the flood event in an ever-growing stratigraphic section of flood sedimentation units. The time of deposition of individual paleoflood slackwater units can be derived by radiocarbon dating of organic matter deposited with the sediment. Fine-grained organics, commonly found at the top of a unit, provide the most accurate estimate of the flood because larger material such as a log may have been eroded from older flood sediments and redeposited by younger events (Kochel and Baker 1982, 1988). Waythomas and Jarrett (1994) also discuss other criteria for distinguishing between coarse-grained paleoflood sedimentation units, including lichen cover, position, clast weathering, and cover by colluvium.

Slackwater sediments can be used to estimate paleoflood stage by tracing a given unit up a tributary canyon and projecting its highest or terminal elevation back to the main valley (fig. 5.37). Experiments by Kochel and Ritter (1987) and field observations during historical floods indicate that these deposits provide a close approximation of the true paleoflood stage. Paleoflood stage information can be used to compute paleoflood discharge using a number of methods. The most common is combining the paleoflood stage information with channel cross-sections and profiles to model the paleoflood flow characteristics using the step-backwater method (Hydrologic Engineering Center 1982). For examples of this see O'Connor and Webb (1988); Baker (1987); Baker and Pickup (1987); and Jarrett (1991). New applications of statistical methods have made the use of discharge-censored data, such as minimum paleoflood stages, even more attractive (Stedinger and Cohn 1986; Stedinger and Baker 1987).

Slackwater deposits have been used to extend flood frequency curves over periods of 2000 to 10,000 years and have been used in a broad range of climatic zones (Moss and Kochel 1978; Patton and Dibble 1982; Kochel et al. 1982; Yang and Xie 1997; Kochel and Parris 2000). When used in conjunction with the historical record, paleoflood data can provide realistic estimates of major floods that plot as *outliers* on flood frequency plots (see fig. 5.35) like that for the Pecos River (Kochel 1988). In this case, conventional statistical techniques for estimating flood frequency applied in 1980 provided estimates of the recurrence interval of the 1954 flood on the Pecos River ranging from 81 years to approximately 10 million years (Kochel and Baker 1982). With the inclusion of slackwater paleoflood data (fig. 5.38) in the analysis the estimated recurrence interval is revised to approximately 2000 years, which is a more reasonable value utilizing both the historical and stratigraphic record of flooding (Kochel et al. 1982).

Although a certain amount of error is associated with all of the paleoflood hydrologic methods (errors can be minimized through careful selection of field sites), they enable hydrologists to make reasonable estimates of the recurrence intervals for large, infrequent floods and are now frequently used as resources in planning decisions. Baker et al. (1987) used slackwater deposits to conclude that overdesign of flood control projects in Arizona's Salt River would be unwise given a record of Holocene flooding spanning thousands of years. Cooley (1990) applied paleoflood techniques to alluvial streams in Wyoming to improve flood frequency

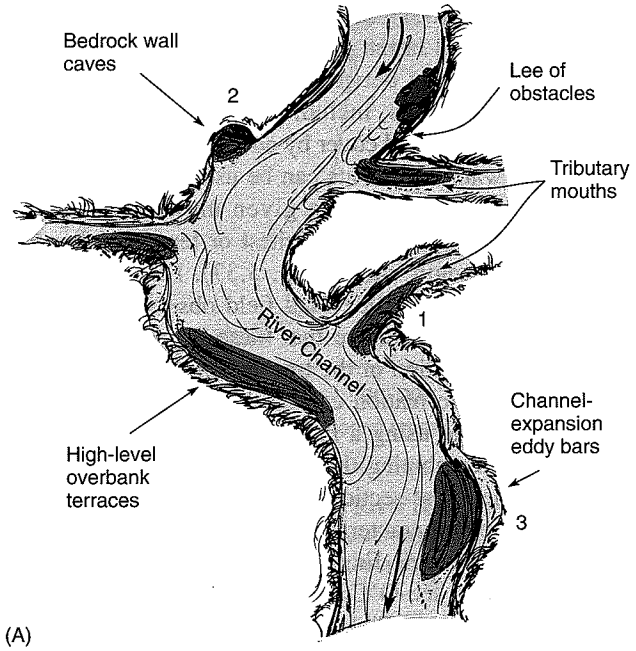

(A)

(B)

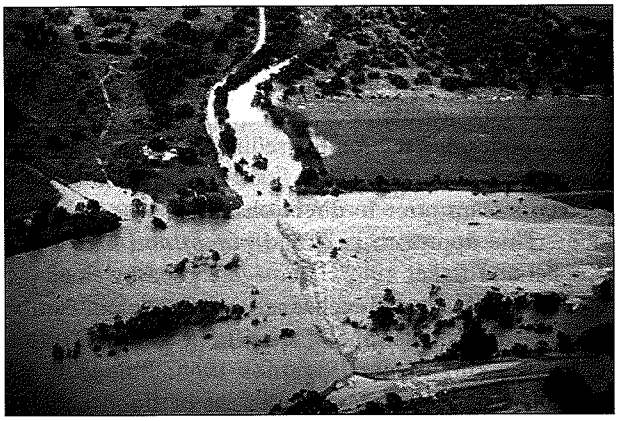

(A1)

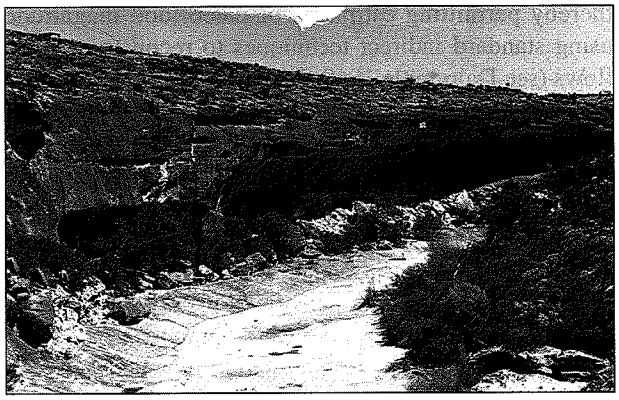

(A2)

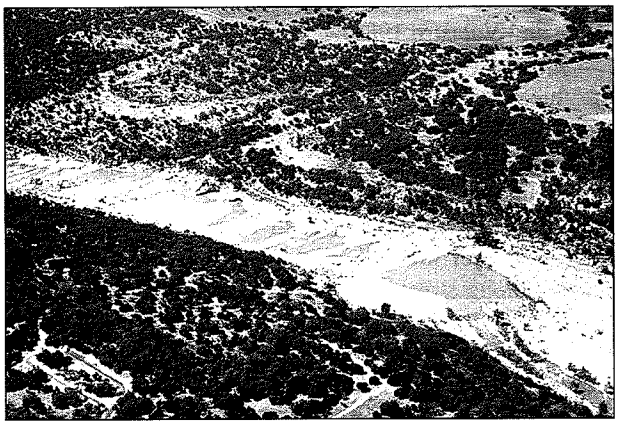

(A3)

Figure 5.36
Slackwater deposits. (A) Location of common sites for slackwater sediment accumulation and preservation. Locations 1, 2, and 3 are illustrated by photos from the Pecos River in southwest Texas. (B) Stratigraphic package of over 2000 years slackwater sediment in a tributary mouth site along the Pecos River. Some of the flood units contain logs and other organic material useful in dating paleoflood events.

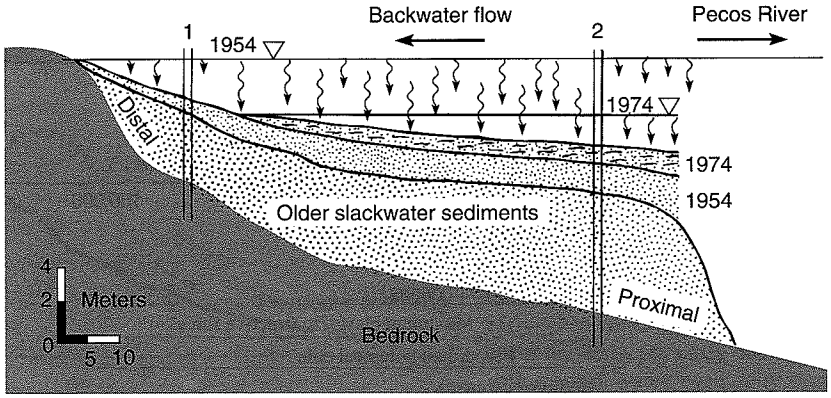

Figure 5.37
Schematic of on- and off-lap sequences and peak flood stage in a tributary valley for the 1954 and 1974 floods on the Pecos River, Texas. Sections in the proximal region (area 2) contain both floods, while distal regions (area 1) farther up the tributary record only the larger 1954 flood. Paleostage reconstructions are based on the elevation of the most distal sediments of each flood unit.
Kochel et al. 1982

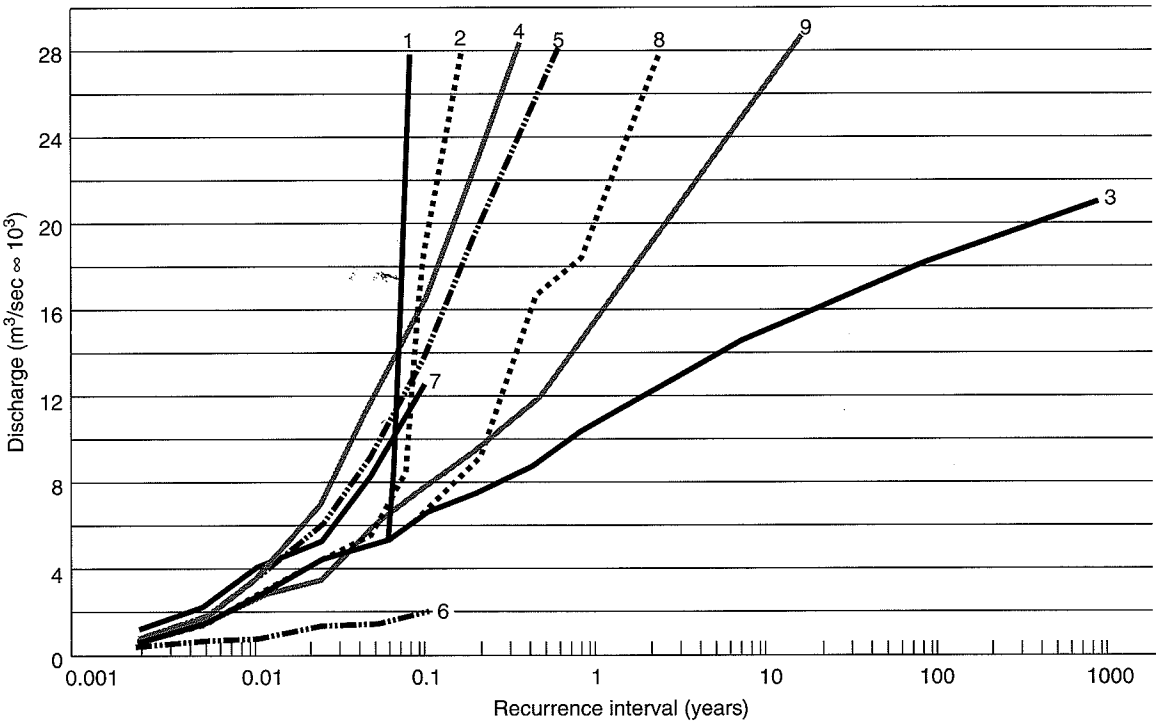

1 (n+1)/m with outliers
2 (n+1)/m historical data
3 (n+1)/m without outliers
4 log Pearson III (outliers, calculated skew)
5 log Pearson III (outliers, regional skew)
6 U.S.G.S. 1977 (1954 contributing area)
7 U.S.G.S. 1977 (entire Pecos drainage)
8 slackwater sediments
9 modified log Pearson (slackwater)

Figure 5.38
Range of potential flood frequency curves calculated using a variety of common standard techniques applied to the Pecos River flow data. Estimates of flood frequency for the 1954 flood outlier range from less than 100 years to more than 20 million years. Slackwater paleoflood deposits were used to provide a more realistic estimate based on physical flood evidence of around 2000 years.
Kochel and Baker 1982

TABLE 5.6 Common Methods for Estimating Paleofloods.

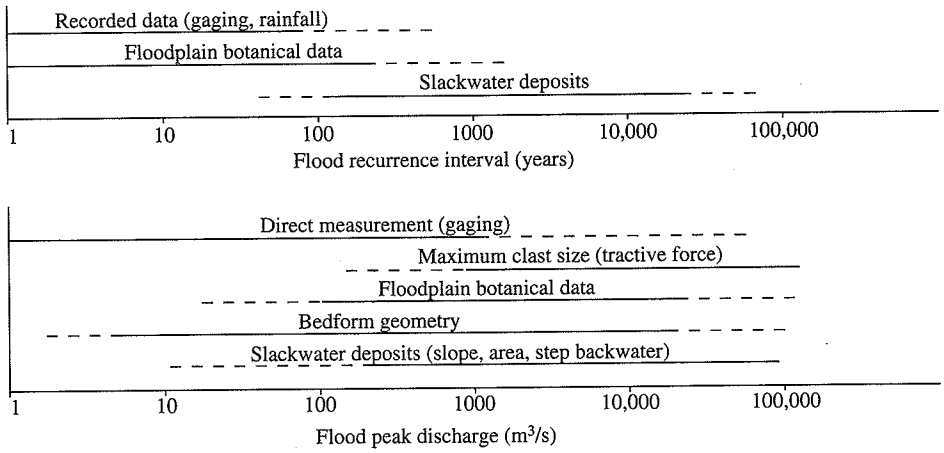

curves used in highway design. Successful techniques used in the Wyoming study included study of terraces, slackwater deposits, debris lines, dendrogeomorphology, and soils. Table 5.6 provides a summary of common paleoflood techniques and the range of applications.

A tremendous explosion in research related to paleohydrology has occurred since Schumm's (1965) seminal paper focusing attention on the prospects for Quaternary paleohydrologic studies (see, for example, entire books dealing with paleohydrologic studies such as Gregory 1983; Starkel et al. 1991). Paleohydraulic flood reconstructions have been used to gain perspective on the magnitude of some of the most catastrophic flows experienced in the Quaternary record such as the great Missoula floods responsible for carving the Channeled Scablands of eastern Washington (Baker 1973; Baker and Nummedal 1978; O'Connor and Baker 1992) and similar glacial lake-related floods in Siberia (Baker et al. 1993). Similar techniques have been used to detail the hydrology of Pleistocene lakes and breakout floods associated with the midcontinent portion of the Laurentide ice sheet (Kehew and Lord 1986; Lord and Kehew 1987).

Paleohydrological techniques also promise to play a major role in assessing the impact of human modifications on global climate, by facilitating the reconstruction of Holocene hydrologic regimes. Recent research has focused on fluvial responses to climatic change. This work is being done in arid bedrock channels (O'Connor et al. 1994) as well as in alluvial channels in semiarid regions (McQueen et al. 1993) and humid climates (Knox 1993; Patton 1988; Martin 1992). Paleoflood studies have been able to elucidate connections between climate and hydrology (Hirschboeck 1987) as well as the spatial variations in flooding between small basins (Martinez-Goytre et al. 1994). Ely (1997) found significant correlations in the frequency of Holocene paleofloods with climate fluctuations in the American southwest. Knox (1993;

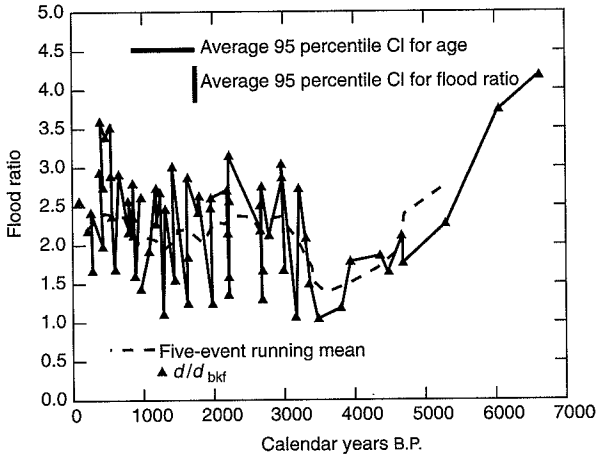

Figure 5.39
Holocene flood variations in the upper Mississippi River basin in response to small variations in climate.
(From Knox 1993)

Knox and Kundzewicz 1997) presented a detailed reconstruction of paleofloods for the upper Mississippi River showing distinctive hydrologic variations during the Holocene. His data indicate that a drier and warmer climate prevailed from 5000 to 3300 B.P. Since then it has been cooler and wetter with more frequent large floods, perhaps similar to the devastating high water experienced in the summer of 1993 (fig. 5.39). Regional and even global correlations are now beginning to appear in paleoflood syntheses (Ely and Baker 1990; O'Connor et al. 1994; Smith 1992; Baker et al. 1995 Gregory et al. 1995; Kale et al. 1997) indicating that these methods may be able to function as useful tools for reconstructing hydroclimatic variations during the Holocene. The apparent correlation of regional paleoflood events with climatic variations should be anticipated because of the

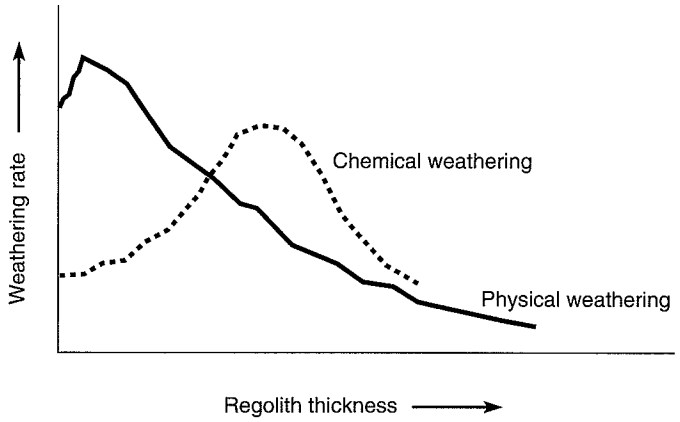

Figure 5.40
Variation in weathering rates as a function of regolith thickness over time. Physical weathering is most effective early when cover is minimal. Chemical rates increase as cover thickens, primarily due to increased time for reaction with regolith water, eventually slowing as thickening cover retards downward movement of water.

high sensitivity of the hydrologic system to climate change (Barron et al. 1989).

Basin Denudation

In addition to being fundamental hydrogeomorphic entities, basins are also geographic compartments where sediment is manufactured, eroded, and deposited, and from which, given sufficient time, the debris will ultimately be removed. The amount of sediment leaving a basin can be readily converted to an estimate of lowering of the basin surface, called **denudation,** which is usually expressed as a time parameter or rate. Denudation seems to have no rigorous definition, but because it implies removal of basin material, it is commonly used as a synonym for erosion. The two processes differ, however, in that denudation refers only to those eroded products that are removed completely from the basin. Considerations of denudation also assume that the sediment is derived in equal portions from all subareas of the watershed and thus, that there is an equal lowering of the surface over the entire basin. Denudation rates tell us little about those erosive processes that simply redistribute sediment *within* the basin, and they do not account for the fact that at any given time some parts of the basin are probably aggrading rather than eroding. Denudation is the long-term sum of the overall erosive process, and even though it is analogous to erosion, it is not precisely the same. Furthermore, the basin surface may not actually lower even with a high denudation rate if active uplift of the basin is proceeding at a greater rate.

Estimates of modern denudation are usually based on measurements of stream load made at gaging stations or on the volume of reservoir space lost when sediment accumulates behind a dam. All types of load (suspended, bed, and dissolved) are included in the analyses at gaging stations, which require that the weight values of the load be converted to volumetric terms. Once the volume of sediment and chemical load leaving the basin is known, it is divided by the area of the watershed above the gaging station to find the vertical dimension, which represents the amount of surface lowering (for details see Ritter 1967). Rates are commonly expressed in inches or centimeters per 1000 years. The type and volume of solid load has a tremendous influence on river behavior. Thus, we must examine the mechanism by which slopes are eroded and what factors affect the mode and rate of the erosive processes.

Slope Erosion and Sediment Yield

The linkages between erosion-sediment yield and the weathering processes (discussed in chapters 3 and 4) are many. Gilbert (1877) introduced a method of analyzing hillslope denudation using mass balance upon which many later investigators have built (e.g., Ahnert 1987). Weathering rates (fig. 5.40) are obviously influenced by regolith thickness because cover thickness regulates water flux to the parent material (important in chemical weathering reactions) and determines the efficacy of frost action on fresh bedrock. Regolith thickness in turn is regulated by denudation processes responsible for removing weathering products, thus illustrating the complex system of feedbacks operating to ultimately determine regolith thickness (fig. 5.41).

Hillslope morphology is a function of the complex interaction of relief-gravity processes, solar radiation, precipitation, kinetic energy, and the resistance properties of the surface, including vegetation cover and shear strength of the regolith (Brandt and Thomas/Thornes 1987). A raindrop possesses a considerable amount of kinetic energy, derived from its mass and the velocity it attains during its fall. Under the influence of gravity, a raindrop accelerates until its force is equal to the frictional resistance of the air, the speed at that point being the *terminal velocity.* As the distance needed to attain this condition is very short, most rain strikes the surface at its terminal velocity, although its absolute speed varies with wind, turbulence, drop size, and so on. In high-intensity rains, drops usually reach a maximum size of approximately 6 mm and a terminal velocity of

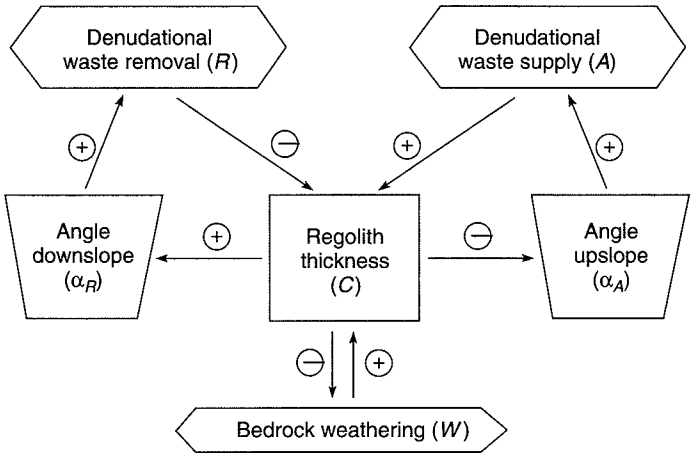

Figure 5.41
Schematic mass balance for denudation in a watershed.
(Ahnert 1987)

about 9 m/s. The impact of such rain can directly displace into the air particles as large as 10 mm in diameter and, by undermining downslope support, can indirectly set even larger pebbles in motion.

The amount of soil moved by splash depends on several interrelated factors. First, the kinetic energy of raindrops is directly related to splash movement (Kneale 1982). However, the kinetic energy of raindrops sometimes varies in unexpected ways. For example, Mosley (1982) found that rain passing through a forest canopy had greater total kinetic energy than normal rainfall and that rainsplash was three times greater under the canopy than in open areas. Second, the type of soil being struck is extremely important in determining the magnitude of splash movement. Free (1960), for example, found that splash loss varied as $E^{0.9}$ for a silt loam and $E^{1.46}$ for a sand, where E is the kinetic energy. Over a five-year period the total splash loss from the sandy surface was calculated at 1600 tons/acre, an amount three times greater than the loss from the loam, probably because the fine-grained soil had greater cohesion. Actually, the manner in which the soil particles aggregate (Luk 1979) and the dispersive properties of the surface material (Yair et al. 1980; Rendell 1982) are more significant controls than simple textural composition. Distinguishing between the energy required for initial detachment of particles and that required to deposit and remobilize them is also important (Hairsine and Rose 1991). Third, the rate and amount of splash transport appear to be a function of slope angle (Savat 1981; Reeve 1982), but the precise relationship is quite variable and not easily determined (Bryan 1979). The effectiveness of rainsplash may also be influenced by the antecedent soil moisture between storms. Rewetting experiments greatly reduced the amount of soil splash by increasing soil shear strength (Truman and Bradford 1990).

In addition to direct transportation, splash has several other erosion-inducing effects on the soil. By detaching particles, it destroys the structure of the soil and breaks apart resistant aggregates of clays. These physical processes make the soil much more susceptible to erosion by surface flow. Furthermore, as splash disperses the clays, they tend to form a fine-grained crust as they settle back on the surface. This crust forms a semipermeable barrier that reduces infiltration and promotes runoff, thereby increasing soil loss by overland flow. Research has shown that aggregate stability may play a central role in regulating rainsplash erosion (Farres 1987). Breakdown of individual soil aggregate appears to be the primary limiting factor in the system. Detailed fieldwork indicates that removal of particles early in a rain event is slow but gradually increase as aggregates begin to break up. Finally, the rate of splash erosion declines again as new crust begins to form (fig. 5.42).

Although the importance of rainsplash in total sediment transport is debated, some studies indicate that the process may be a major component of hillslope denudation. Morris (1986) found that rainsplash accounted for up to 88 percent of the fine-sediment flux during 1982 in a Colorado Front Range drainage basin.

Wash Most natural slopes are too irregular to permit a uniform flow of water, or *wash,* over the entire surface; flow is deeper over depressions and shallower over flat reaches or high spots. The variable depth of flow produces differences in the eroding and transporting capabilities of the water. Wash does not imply that a regular sheet of debris is being carried continuously down the slope surface. In areas where *sheet flow* might be possible, only fine-grained particles can actually be moved efficiently, and those only if the surface has been prepared for erosion by rainsplash or weathering processes that reduce cohesion. In areas of concentrated flow, larger sediment can be moved, but the ability to erode depends more on the hydraulic force of the water and less on the condition of the surface.

When rainfall and flow become intense, small shallow channels may be formed which periodically shift position so that in the long run erosion is more or less even across the slope. In fine-grained soils, a set of well-

alter drastically the natural sediment yield (Moore 1979; Dunne 1979; Toy 1982). Projections of changes in world land use between 1700 and 2000 are shown in table 5.7 (Richards 1990). The magnitude of change between 1950 and 1980 exceeded that between 1700 and 1850.

Evidence indicates that human activities may increase detrital loads by at least an order of magnitude (Judson 1968a; Meade 1969). Chemical loads are also expanded by pollutants introduced into the streams and the atmosphere (Meade 1969). One important contributor to accelerated erosion is the replacement of mature forest cover by intensely cultivated land (Toy 1982; Walling and Quinne 1990; Foster et al. 1990). Studies in the United States show an increase in sediment yield of one to three orders of magnitude when crops are substituted for natural vegetation (Ursic and Dendy 1965; Wolman 1967). With proper soil conservation techniques, however, the effect can be reversed and sediment yield values will decrease dramatically (Trimble and Lund 1982).

Construction associated with urbanization causes an even more dramatic rise in the sediment yield (e.g., Guy 1965), but after construction is completed, the values decrease rapidly (fig. 5.51) because much of the surface is protected from erosion by concrete citadels (Wolman 1967). Urbanization also affects the runoff characteristics within a drainage basin (McPherson 1974); consequently, the concentration of sediment in streams, as influenced by humans, depends on variations in hydrology and sediment yield. In a global review of sediment yields, Walling and Webb (1996) showed that sediment yields have increased since 1964 in most areas. Renwick (1996) suggested that human impact significantly overshadows the natural spatial variation in sediment yields.

Several workers have suggested that the abnormalities induced by human activities may be great enough to invalidate the use of sediment yields to calculate rates of denudation in drainage basins (Douglas 1967; Trimble 1977). Trimble (1977) was able to show that in large drainage basins in the southeastern United States, lowering of upland surfaces was proceeding at a rate of 95 mm/100 yr; in contrast, the denudation rate calculated by sediment in the streams was only 5.3 mm/100 yr. Thus, the *sediment delivery ratio* (sediment yield as a proportion of upland erosion) was only 6 percent. Sediment yield, therefore, may be a poor indicator of how rapidly the upland area of a basin is being lowered. The major portion of sediment eroded from the uplands is, of course, being stored within the basin by deposition. A similar example can be cited from central Virginia, where much of the denudation in small upland watersheds is accomplished by a small number of catastrophic debris avalanche and debris flow episodes occurring at return intervals on the order of thousands of years (Kochel 1987). Much of the sediment denuded from the Virginia hillslopes during these events is temporarily stored in debris fans within the basin.

Meade (1982) has suggested that the accelerated erosion produced by early settlers in the eastern United States while clearing land for cultivation has been largely arrested by soil conservation and reduced acreage of agricultural lands. However, sediment stored in the basins in response to the earlier settlement is now being eroded and is augmenting the present river loads and will continue to do so for decades or centuries to come. Modern river loads may be reflecting erosional events that occurred in the distant past. Considerable literature exists focused on determining the cause of wide-

TABLE 5.7 Global Land Use Changes from 1700 to 2000.

Land Use	Percent Change	Area Change (ha)
Forest/woodlands	−19	−1.2 billion
Grassland/pasture	−8	−560 million
Cropland	+21	+1.2 billion

Source: Richards (1990).

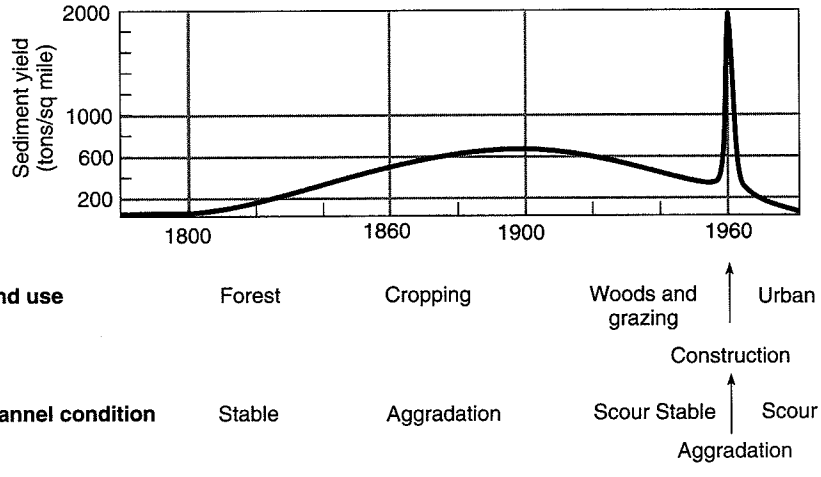

Figure 5.51
Changes in sediment yield and channel behavior in one area under various types of land use.
(Wolman 1967)

spread incision of channels (arroyos) in the American Southwest beginning in the late 1800s. Most arguments fall into two camps—climatic change (precipitation amount and intensity) and overgrazing. Working in the Southern Colorado Plateau, McFadden and McAuliffe (1997) were convinced that arroyo incision would be correlated with climate change. They believe that increased precipitation triggered accelerated erosion of sparsely vegetated slopes.

Characterizating human impact on the landscape is not simple, for the relationships between land use and sediment yield are complex (Foster et al. 1990). As shown in figure 5.52, impacts on hydrology and vegetation can influence geomorphologic and pedologic processes on varying scales of time and space (McDowell et al. 1990). Adding to the difficulty of understanding these human-induced changes is the fact that many adjustments occur in episodes that are regulated by discrete geomorphic thresholds, resulting in complex response phenomena. Before the human impacts can be assessed, the influence of geomorphic phenomena known to operate and influence systems over time scales similar to the period of significant human activity (10–1000 years) must be accounted for. McDowell et al. (1990) suggest that short-term climate change and tectonics may be the most influential of these factors and can sometimes overshadow the impact of human activity. Recent research is beginning to shed some light on the likely responses of geomorphic systems to short-term climatic fluctuations (Kochel and Miller 1997). Studies of lake sediments hold great promise of providing high-resolution records of basinal changes in sediment yield and runoff (Halfman and Johnson 1988; Foster et al. 1990). Recent work by Brown et al. (2000) in Vermont has documented a 10,000-year record of storm-induced sedimentation into northern Appalachian lakes, discernible at reasonably fine resolution.

On the other hand, numerous studies document landscape alterations, such as alluviation and erosion, that are occurring over just several decades (Knox 1977; Goudie 1986; Harvey and Schumm 1987). The complexity, frequency, and magnitude of human impacts are increasing (Goudie 1986). Arguments have long been waged regarding the relative influence of climate change versus land use in the dynamics of arroyo development in the American Southwest. Recent investigations have demonstrated significant climate changes coincident with the timing of arroyo incision and alluviation. The magnitude of these climate changes could impact basin hydrology and sediment dynamics significantly. The argument for climatic causes is strengthened because response has generally been regionally consistent rather than locally variable (for example, see Hereford 1986; Graf et al. 1991; Wells and Meyer 1993; McFadden and McAuliffe 1993).

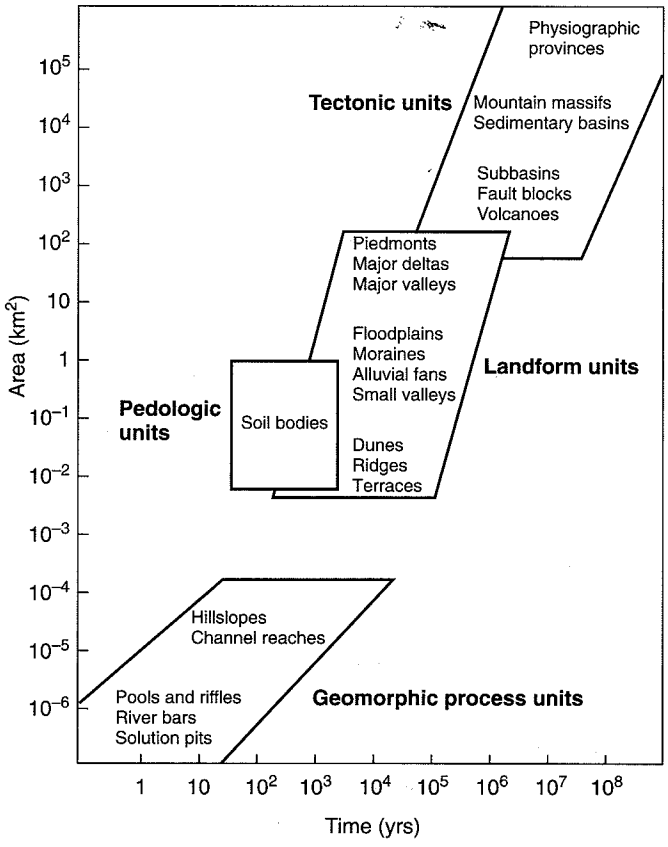

Figure 5.52
Spatial and temporal scales of human impact on geomorphic processes and landforms.
(McDowell et al. 1990)

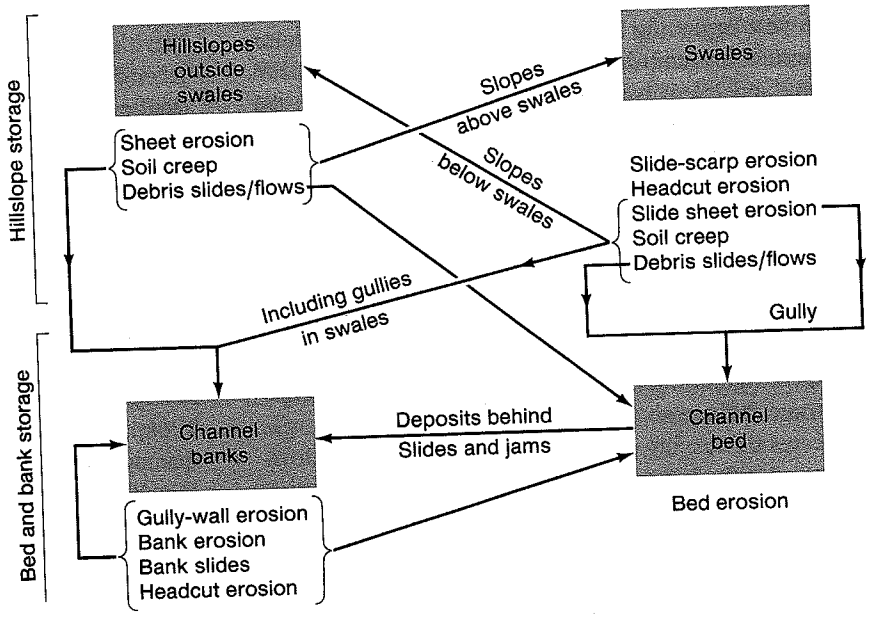

Figure 5.53
General linkages between sediment storage sites and erosional processes. Boxes indicate storage elements; listed below each box are erosional processes mainly responsible for mobilizing sediment in that element. Arrows show transfers between elements. Labels on arrows qualify or restrict location of transfers.
(Lehre 1982)

TABLE 5.8 Sediment Budget for a Small Drainage in Northern California for the Years 1971 to 1974.

			Sediment (metric tons/km2)				
Year	Rainfall (mm)	Recurrence Interval of Peak Flow (yrs)	Mobilization on Slopes (1)	Production to Channels (2)	Redistribution on Slopes (3)	Yield: Bed + Susp. Load (4)	Bed + Bank Storage (5 = 2 – 4)
1971–72	602	1.5	86	148	–71	24	+124
1972–73	1184	15–20	1219	985	+317	1420	–435
1973–74	1046	3–5	1960	1575	+389	630	+945
1971–74	2832	—	3265	2708	+635	2074	+634

From Lehre (1982).

Sediment Budgets

Storage of sediment within a basin is a significant geomorphic phenomenon. Its importance is underscored by the concept of a sediment budget (Dietrich and Dunne 1978; Kelsey 1980; Lehre 1982). A **sediment budget** is a quantitative analysis of a drainage basin that shows the relationship among erosion of basin materials, discharge of sediment from a basin, and the associated changes in sediment storage. In essence, it is an accounting sheet of ins and outs of sediment and as such is similar to the hydrologic budget discussed earlier. Of greater importance, however, is its significance in planning and land management because it distinguishes the dominant erosional processes in the basin and the circumstances under which storage of sediment may change. Additionally, the sediment budget demonstrates the process linkage that we discussed in chapter 1 (fig. 5.53).

To make a complete sediment budget analysis one must identify and quantify *sediment mobilization* (processes that initiate motion and move sediment any distance), *sediment production* (the amount of sediment reaching or given access to a channel), and *sediment yield* (sediment actually discharged from the basin). For example, table 5.8 shows the sediment budget for the years 1971 to 1974 in a small drainage basin northwest of San Francisco (Lehre 1982). In dry years or years without extreme flow events (1971–1972, 1973, 1974), most mobilized and produced sediment was stored within the basin. In contrast, during the year having a flow event with a 15- to 20-year recurrence interval (1972–1973), the amount of sediment mobilized and produced was less than the amount discharged from the basin. This indicates that sediment was taken out of storage during that year, presumably by erosion of channel banks and beds. By continuous observation, Lehre (1982) was able to demonstrate that the variations in annual sediment budgets shown in table 5.8 were accompanied by different erosive processes. In the years of low rainfall and/or peak flow, sediment was mobilized by spalling, rainbeat, and minor sliding and was moved

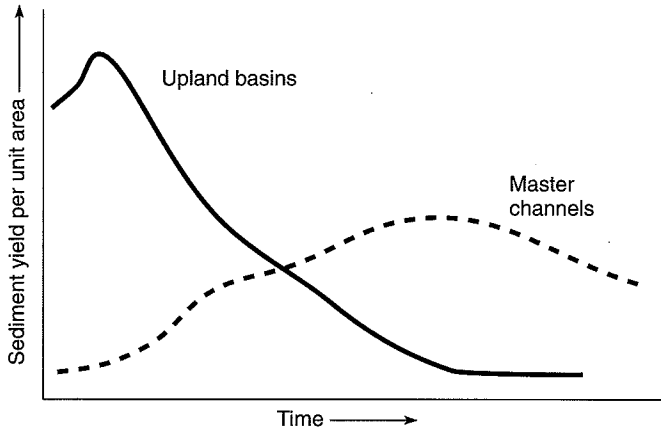

Figure 5.54
Relative timing of sediment movements in drainage basins since the end of Pleistocene glaciation. Note the shift in activity progressively downstream through the system with time.
(Church and Slaymaker 1989)

toward the channels by sheetwash. The lack of water, however, assured a minimum transport distance and most sediment went into storage. In the year of high peak flow (1972–1973), sediment was mobilized and produced mainly by debris slides and flows. It was quickly delivered to the channels and, because of the coincidence of high channel discharge, was removed from the basin.

Sediment budget analysis is a relatively new way of looking at the inner workings of a drainage basin, and we do not yet know what its applications will be. However, it seems to hold considerable promise for land management, especially in small basins that are unstable geomorphically and subject to a variety of interrelated processes.

Recently, there has been a significant upsurge of interest in the dynamics of sediment transfer, such as sediment storage and delivery, through the drainage basin. In particular, studies have focused on the spatial distribution and residence times of sediments because of concern over the location and mobility of contaminants introduced by human activities within the watershed. These studies are beginning to reveal distinctive patterns in sediment storage and distribution along the fluvial system. For example, Florsheim and Keller (1987) observed an inverse relationship between unit stream power (which reflects the ability of a channel to generate stresses necessary to entrain sediments) and the volume of sediment stored along a specific channel reach. Sediments are generally stored upstream and downstream of channel and valley constrictions; they pass through the constricted reaches because of high unit stream power generated there. Many studies have emphasized the importance of episodic erosional events in sediment movement, particularly in small, upland watersheds (Lisle 1987; Grant and Wolff 1991; Jacobsen et al. 1989). Miller et al. (1999) discuss the significance of episodic events in mobilizing flood plain sediment containing heavy metal contaminants from 19th-century mining during a major flood on the Carson River in Nevada in 1997. Church and Slaymaker (1989) have shown that many basins in areas that experienced Quaternary glaciation may still be attempting to adjust to dramatic increases in sediment input delivered immediately after a glacial interval (sometimes referred to as paraglacial), some 10,000 years ago. Figure 5.54 demonstrates the delay in sediment transfer in response to this paraglacial sedimentation from upland basins to downstream areas along the master channels envisioned in montane areas of the Canadian Rockies.

Another generalization from studies of sediment yield and delivery indicates that the sediment delivery ratio varies systematically through a basin from headwater on downstream regions. Sediment delivery ratios are generally high, in excess of 90 percent (Trimble 1977), for upland, low-order watersheds, while they may be as low as 4 percent by the time coastal plain areas are reached (Phillips 1991). Recent advances in the use of cosmogenic isotopes such as ^{10}Be, ^{137}Cs, and Cl for dating are beginning to improve efforts to quantify sediment transfers. For example, Brown et al. (1988) showed that only a small portion of the volume of sediment mobilized from hillslopes ever leaves the basin. Considerable perturbation of expected natural patterns and rates of sediment storage and transport can occur due to the impact of artificial channelization along alluvial reaches (Simon 1989).

Sediment yield has long been known to be an important signal of tectonic, base-level climatic change in fluvial systems (i.e., Schumm 1977; Bull 1991). Chumm and Rea (1995) viewed sediment-yield patterns from areas disturbed by changes in the above parameters and found that they all result in increases in sediment yield at all scales from small experimental to the Himalayan Basin. However, they also found that if no further disturbance occurs, sediment yields will lower rapidly as the systems reestablish equilibrium. Interpretations of sediment yield promise to continue to be an important tool for interpreting the record of past adjustments of climate, base level, and tectonics.

Rates of Denudation

In spite of the problems inherent in analyzing denudation rate, various estimates have been made (fig 5.55). Table 5.9 presents a random sample of modern denudation rates for basins of varying size in the United States. The values are imprecise and probably high because in most cases they do not include an adjustment for human impact. Nonetheless, they do indicate a general tendency for denudation rates to fall between 2.5 and 15 cm per 1000 years when considered on a regional scale. Judson (1968b) recalculated the denudation rate for the entire continental United States by subtracting the effect of human occupancy from earlier estimates. His figure of 3 cm per 1000 years agrees rather closely with the denudation in very large drainage basins that are mostly unaffected by anthropogenic disturbance (Gibbs 1967) and perhaps represents a reasonable approximation for denudation on a continental scale.

Although methods other than analyses of sediment wedges have been employed (Eardly 1967; Ruxton and McDougall 1967; Clark and Jager 1969), most rates of denudation have been estimated from measurements of sediment accumulation in depositional basins. A valid estimate can be made only if (1) the volume of sediment derived by erosive processes can be accurately determined, (2) the boundaries of the source area are defin-

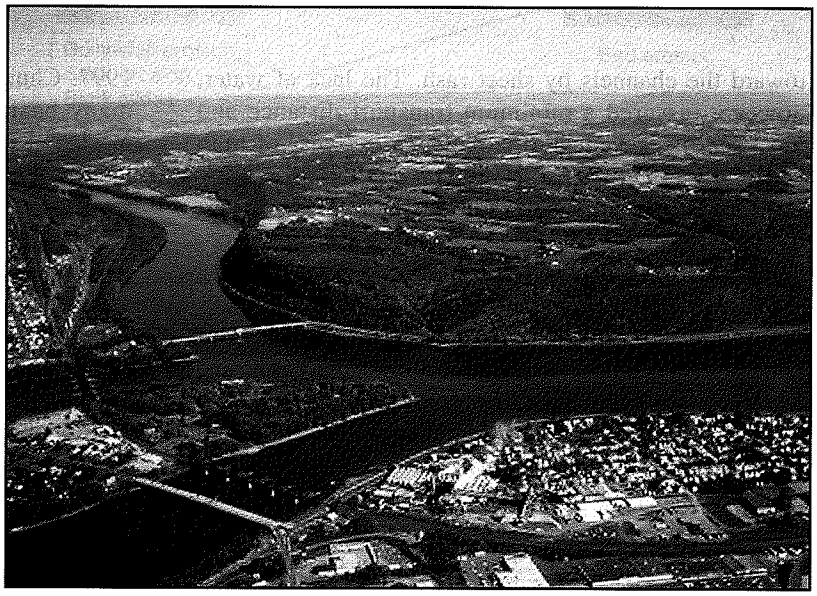

Figure 5.55
Junction of the main branches of the Susquehanna River at Sunbury, PA. Note the plume of suspended sediment emanating from the main branch, which recently experienced a rainfall. Water from the west branch (left) is relatively clear.
(Photo by R. Craig Kochel)

TABLE 5.9 The Influence of Geology and Climate on Suspended-Load Denudation in Basins of Different Size in the United States.

Basin	Location	Area (mi^2)	Average Annual Suspended Load (tons $\times 10^3$)	Denudation (in/1000 yr)
Mississippi	Baton Rouge, La.	1,243,500	305,000	1.3
Colorado	Grand Canyon, Ariz.	137,800	149,000	5.6
Columbia	Pasco, Wash.	102,600	10,300	0.5
Rio Grande	San Acacia, N.M.	26,770	9,420	1.8
Sacramento	Sacramento, Calif.	27,500	2,580	0.5
Alabama	Claiborne, Ala.	22,000	2,130	0.5
Delaware	Trenton, N.J.	6,780	998	0.8
Yadkin	Yadkin College, N.C.	2,280	808	1.8
Eel	Scotia, Calif.	3,113	18,200	30.4
Rio Hondo	Roswell, N.M.	947	545	3.0
Green	Palmer, Wash.	230	71	1.6
Alameda	Niles, Calif.	633	221	1.8
Scantic	Broad Brook, Conn.	98	7	0.4
Napa	St. Helena, Calif.	81	63	4.1

Data from Judson and Ritter (1964).

able, and (3) the time interval of sediment accumulation can be ascertained within reasonable limits. It is very difficult to meet all these requirements. Noneroded matter such as pelagic and volcanic rocks add to the depositional volume, material eroded from the basin as dissolved load may not be returned to the deposit by chemical precipitation, and absolute dates that bracket the time of deposition are necessarily imprecise. Nonetheless, some estimates of past rates have been made for large portions of North America (Gilluly 1949, 1955, 1964; Menard 1961). It is interesting to note that the rates found in these studies of large regions are within the same order of magnitude as those based on modern stream data. This similarity prompted the hypothesis (Ritter 1967) that when viewed on a large enough area or over a long enough time interval, denudation rates will probably be about the same. Based on current evidence, the average value will probably fall somewhere between 2.5 and 15 cm per 1000 years. That range is generally supported by estimates of solid and dissolved loads being delivered to the oceans from the world's continents (table 5.10). Estimates of total denudation must include chemical as well as solid loads if they are to be reliable over the long term. For example, Sevon (1989) found that denudation rates ranged only from 10 m per million years from historical stream sampling to 27 m per million years based on analyses of the long-term stratigraphic record for the Juniata River (a major tributary to the Susquehanna River in central Pennsylvania). These estimates, although different, are certainly in the same ballpark. The advent of new Quaternary dating technologies such as ^{137}Cs will undoubtedly yield improved estimates of continental erosion rates (Walling and Quine 1990).

The use of denudation rates for continent-sized areas (table 5.10) can lead to erroneous conclusions. For example, a 3 cm/1000 yr rate suggests that 300 m of surface lowering will be accomplished over an entire continent in a 10-million-year period. Such a rate might be used as evidence to support the generally accepted canon of geomorphology that most of the topography of Earth is no older than Pleistocene, meaning that almost all landscapes formed in the last 2 million years. Therein lies the fallacy of denudation rates, because we know that large regions of Tertiary and older landforms do exist, especially in the Southern Hemisphere. For example, radiometric dates and geologic evidence in southeastern Australia show that much of that landscape was in its present form by the mid-Miocene, and some upland surfaces originated in the Mesozoic (Young 1983). The inconsistency of these observations with denudation analyses from river sediment arises because denudation rates are unrealistically spread over entire continents. Actually, the interiors of continental plates probably experience extremely slow denudation and may easily preserve old landscapes (Young 1983). In contrast, continental plate margins where active tectonism is occurring probably have enormously high denudation rates. Combining the two subareas provides an average rate for the continent that is indicative of neither. The point here is that a denudation rate calculated for a large basin or region tells us nothing about the tenor of erosion occurring in any component part of that basin, and the overall rate should never be used in that sense. Romero-Diaz et al. (1988) illustrated how great the spatial variation in denudation rates can be between local areas.

McLennan (1993) maintains that a general relationship exists between sediment yield and major denudational regions of the world when considered in regard to weathering history (table 5.10). Weathering history is recorded in the major element composition of suspended sediments. In this scheme, equilibrium denudational regions are areas that have a sediment yield that is in equilibrium with existing dominant weathering conditions. On the other hand, nonequilibrium denudational region areas have sediment yields generally much lower than predicted. Often, such anomalies are related to sediments trapped in lakes such as the Great Lakes system (McLennan 1993).

TABLE 5.10 Denudation Estimates Based on Solid and Dissolved Loads Delivered to the Ocean by Major Rivers of the Continents.

Continents	Solid Load ($t/km^2/yr$)[a]	Dissolved Load ($t/km^2/yr$)[b]	Total Load	Denudation Rate (cm/1000 yr)
North and Central America	84	33	117	4.00
South America	97	28	125	4.28
Europe	50	42	92	3.15
Asia	380	32	412	14.10
Africa	35	24	59	2.02
Australia	28	2	30	1.03

[a]Solid load from Milliman and Meade (1983).

[b]Dissolved load from Garrels and Mackenzie (1971).

SUMMARY

In this chapter we examined a remarkable statistical balance between the spatial characteristics of river networks and the watersheds that contain them. Because the parameters of this morphometry also relate in a significant way to the hydrologic and erosional properties of most watersheds, drainage basins serve as primary units for systematic analyses of geomorphology. Drainage basins and river networks probably evolve according to fundamental hydrophysical laws, but their ultimate character is conditioned by the geological framework and the external constraints of climate. An equilibrium condition, defined in terms of mathematical balance, is probably attained early in the growth history of most basins. This does not mean, however, that basins evolve in an orderly way with time. Geologic catastrophes that upset equilibrium tend to be filtered out in a morphometric sense because basinal parameters apparently adjust to changes rather quickly.

Water flowing in basin rivers is derived from variable sources, and sediment reaching stream channels is produced and delivered by numerous erosive processes operating on basin slopes. Both water and sediment are amenable to budget analyses, which provide basic data for watershed planning. The amounts of water and sediment entering stream channels are functions of the physical properties of the basin and the effect produced by human activities. Estimates of basin denudation can be made on the basis of total sediment yield, but difficulties are created by sediment storage within the basin. The following references provide greater detail concerning the concepts discussed in this chapter.

SUGGESTED READINGS

Baker, V. R., Kochel, R. C., and Patton, P. C., eds. 1988. *Flood geomorphology.* New York: John Wiley and Sons.

Dunne, T., and Leopold, L. B. 1978. *Water in environmental planning.* New York: W. H. Freeman.

Fetter, C. W. 1994. *Applied hydrogeology.* Columbus, Ohio: Merrill.

Gregory, K. J., and Walling, D. E. 1978. *Drainage basin form and process.* New York: Halsted/John Wiley.

Kochel, R. C., and Miller, J. R. 1997. Geomorphic responses to short-term climate change. Special Issue, *Geomorphology* 19:170–368.

Mayer, L., and Nash, D. 1987. *Catastrophic flooding.* Boston: Allen and Unwin.

Rhodes, B. 1992. Fluvial geomorphology. *Progress in Physical Geography* 16:489–96.

Schumm, S. A. 1977. *The fluvial system.* New York: John Wiley.

Schumm, S. A., Mosley, M. P., and Weaver, W. E. 1987. *Experimental fluvial geomorphology.* New York: John Wiley.

Singh, V. P. 1987. *Regional flood frequency analysis.* Dordrecht: D. Reidel.

Turner, B. L., Clark, W. C., Kates, R. W., Richards, J. F., Mathews, J. T., and Meyer, W. B., eds. 1990. *The earth transformed by human action.* Cambridge: Cambridge Univ. Press.

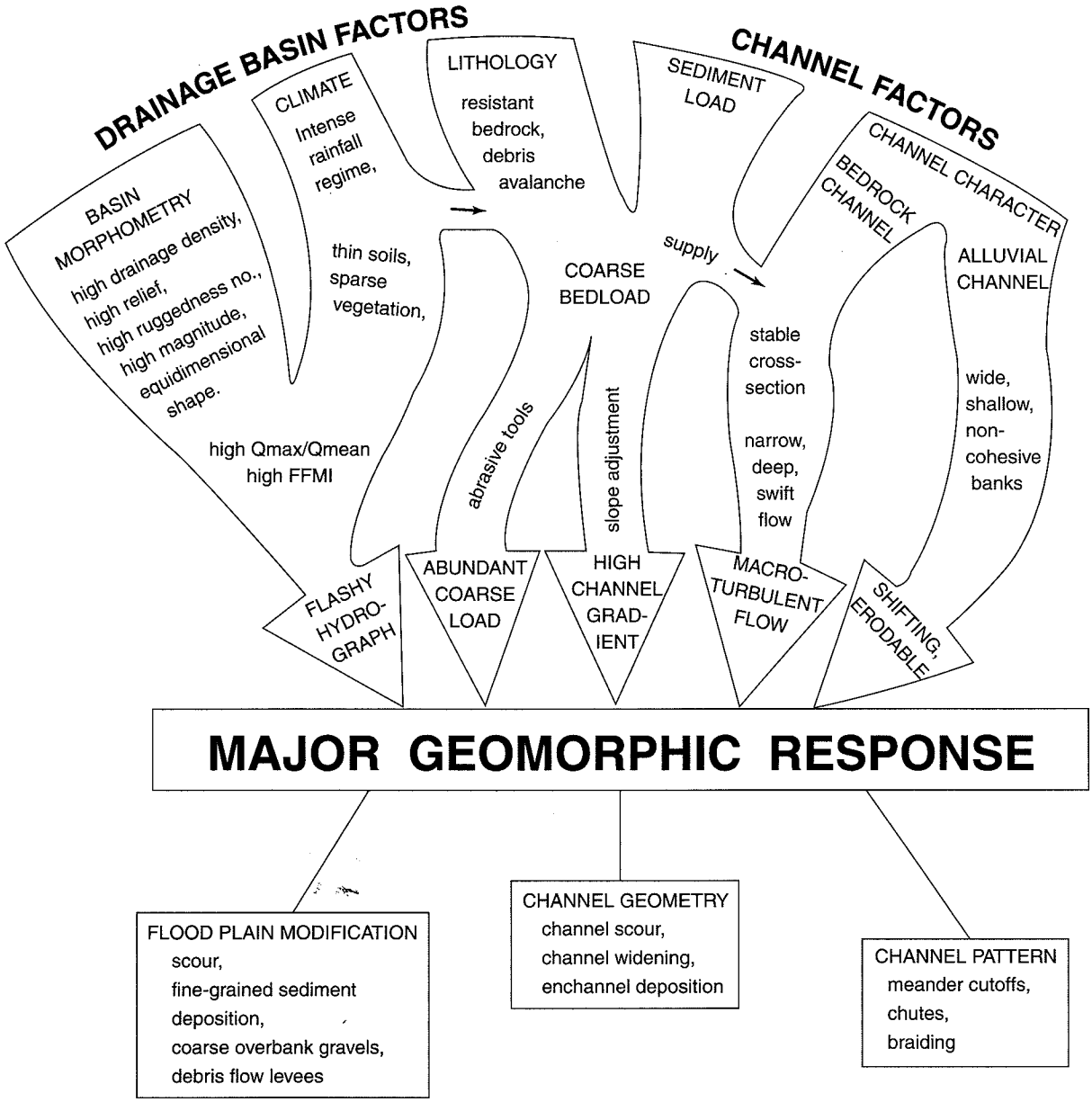

Figure 6.16
Summary of the factors controlling channel and floodplain response to large-magnitude floods.
(From Kochel 1988)

Hydraulic Geometry

The quasi-equilibrium condition was first demonstrated in a landmark study by Leopold and Maddock (1953). Using abundant flow records compiled at gaging stations throughout the western United States, they set out to determine the statistical relationships between discharge and other variables of open channel flow; these relationships are known as *hydraulic geometry* of river channels. Because every river has wide fluctuations in discharge, any given channel cross-section must transport the range of flows that comes to it from the adjacent upstream reach. Discharge, therefore, serves as an independent variable at any station, and the changes in width, depth, velocity, or other variables can be observed over a wide spectrum of discharge conditions (fig. 6.17). At a station each of the factors (w, d, v) increases as a power function such that

$$w = aQ^b$$

$$d = cQ^f$$

$$v = kQ^m$$

where a, c, k, b, f, and m are constants. The exponents b, f, and m indicate the rate of increase in the